Master's Thesis

A Geometric Feature-based Stress and Deformation Estimation Model for Optimal Assembly Part Positioning on Transformable Pin-jigs

Jongil Park

Department of System Design and Control Engineering

Graduate School of UNIST

2018

A Geometric Feature-based Stress and Deformation Estimation Model for Optimal Assembly Part Positioning on Transformable Pin-jigs

Jongil Park

Department of System Design and Control Engineering

Graduate School of UNIST

A Geometric Feature-based Stress and Deformation Estimation Model for Optimal Assembly Part Positioning on Transformable Pin-jigs

A thesis/dissertation
submitted to the Graduate School of UNIST
in partial fulfillment of the
requirements for the degree of
Master of Science

Jongil Park

06. 12. 2018

Approved by

Advisor
Duck-Young Kim

A Geometric Feature-based Stress and Deformation Estimation Model for Optimal Assembly Part Positioning on Transformable Pin-jigs

Jongil Park

This certifies that the thesis/dissertation of Jongil Park is approved.

06. 12. 2018

Advisor: Duck-Young Kim

Sung-Youb Kim

Namhun Kim

Abstract

Recently, the increasing demand for customization, innovative products, and the rapid change in customer demands have resulted in shorter product lifecycles and more cost effective technologies. As a result, the recent trend in manufacturing is to use reconfigurable manufacturing systems for providing a cost effective and rapid response to customer demands. With regard to jigs, a reconfigurable jig is necessary to achieve reconfigurability of entire system. Therefore, a reconfigurable jig with computer-aided design and finite element analysis is introduced. Unlike conventional jigs, the reconfigurable jig can change its shape depending on the shape of the product. The reconfigurable jig was implemented using pins. In this study, the reconfigurable jig system is designed for the process of assembling the car door inner modules. Because the pin-jig can be adjusted in terms of size or spacing, it can be applied to products of various sizes. Therefore, it can be used to build a reconfigurable manufacturing system.

However, the problem with traditional pin-jig is that the initial product placement is visually ambiguous and insufficient in quality compared to existing jigs. In order to solve these problems, many researchers have used computer-aided design to acquire visual assistance. In addition, the computer-aided design helps in automatically calculating the strokes of pin-jigs. To evaluate the quality of a product, some experiment was conducted by applying finite element analysis to the product and pin-jigs. The method to evaluating the quality of a product involves analysis of the stress and deformation of a product according to the shape of the product. From the result of finite element analysis, the shapes were prioritized to decide the best location for the product. These methods help the reconfigurable jig to locate the product appropriately. In addition, an assistance method to locate a part with a geometric feature-based stress and deformation estimation model for optimal assembly part positioning were developed.

Table of Contents

List of Figures

List of Tables

I. Introduction

In the past, industries have mostly focused on reduction of manufacturing costs and mass production. Recently, the increasing demand for customization, innovative products, and the rapid change in customer demands have resulted in shorter product lifecycles and more cost effective technologies (Yang, Gao, Simon, Zhu, & Su, 2018). As a result, the recent trend in manufacturing is to use reconfigurable manufacturing systems for a cost effective and rapid response to customer demands (Koren & Shpitalni, 2010).

A traditional jig is made by cutting a rigid material and its shape is changed according to the type of product. Therefore, jigs of various shapes need to be installed in each process line. In the case of the assembly process for the car inner modules, the process line has five fixed-shape mono-cast-nylon jigs, fixed on a thick plate. Therefore, even if the shape of the product is slightly changed, the existing jigs should be discarded and replaced with new jigs.

The installed jigs will also have to be idle if there is insufficient demand for a product. Moreover, the jig design is based on expert knowledge and is a very time-consuming process. The cost of redesigning, manufacturing, and installing a fixture is about $100 million/plant/year in the case of automotive manufacturing (Bone & Capson, 2003). Reconfigurable manufacturing systems and flexible manufacturing systems that can follow the rapid changes in customer demand could reduce both cost and lead time (Jonsson & Ossbahr, 2010).

Developing a reconfigurable fixture is one of the processes in the design of reconfigurable manufacturing systems. Most of the manufacturing processes involve fixing, supporting, and locating a product using fixtures. Designing and manufacturing fixtures is one of the most costly and time-consuming processes in product industrialization. In fact, redesigning, manufacturing, and installing a fixture accounts for about 10–20% of the total manufacturing cost (Jonsson & Ossbahr, 2010). Moreover, reconfigurable fixtures can be used for a variety of products (Simon, Kern, Wagner, & Reinhart, 2014).

Various theories and approaches related to the design of fixtures have been introduced in order to study the manufacture reconfigurable fixtures (Wang et al., 2010; Cecil, 2001; Boyle et al., 2011). However, most of these researches have focused on the physical shape of the fixture regardless of the external forces applied to a part. For a more effective and defect-free manufacturing system, the effects of external forces should be researched.

Typically, a fixture has two mechanical parts, namely locator and clamp. A jig that can be classified as a locator takes a reaction force depending on the external force. Therefore, there are location issues when a part is flexible and deformable (Fuwen, 2014). In order to reduce the formation of defects in a product, the position of the product should be considered in the presence of external forces in the assembly process.

The problem with the traditional pin-jig is that the initial product placement is visually ambiguous and insufficient in quality compared to the existing jigs. Most researchers have not covered the human perception issue when placing parts on reconfigurable fixtures or jigs (Molfino, Zoppi, & Zlatanov, 2009; Munro & Walczyk, 2007; Simon et al., 2014). Therefore, this paper aims to provide the readers a clear solution to the two preceding problems. Using the software, the user will be able to preview in 3D which product needs to be mounted, and where.

From the point of view of an inner car part, we developed a transformable jig system in which the shape of the discrete pin-jigs can be reconfigured according to the 3D CAD model of part. The pin tooling fixture, which is one type of adaptive fixture, has the following benefits (T.Patil, S.M.Pise, S.G.Bhatwadekar, & S.B.Sangale, 2015):

- Pin-jig reduces the design and development time of new jig.
- Pin-jig reuses the existing fixture data to the maximum possible extent while generating a reconfigurable manufacturing system, thus reducing cost of developing a new fixture.
- Pin-jig reduces the lead-time and overhead cost by storing and retrieving multiple fixtures.

A motorized multi pin-array jig can support more pressure against an external force and can adjust the height of pin-jigs more sophisticatedly than pneumatic pin-jigs (Olaiz, Zulaika, Veiga, Puerto, & Gorrotxategi, 2014). However, their complexity of implementation and cost are greater than those of mechanical pin-jigs are (Peters, 2013).

In addition, an automated jig system for the assembly line should consider external forces. The effect of external forces reduces the quality of the product. Because of the fixed interval between each pin-jig, a deflection or displacement may occur when the potential energy of the part is not in an equilibrium state (YAMADA, YAMADA, & YAMAMOTO, 2011). A finite element method could predict such deflection or displacement in advance. However, the finite element analysis is not suitable

for reconfigurable systems, because the finite element method cannot give the solution instantaneously when the target part has a huge size.

The development of reconfigurable manufacturing systems requires a control system and a physical system (Xuemei, 2009). In this study, a reconfigurable pin-jig system that consists of a transformable pin- jig (physical system) and a 3D pin-jig shape transformer (control system) is developed for implementing the reconfigurable jig. The testbed for this system is the assembly line of an inner car part. Therefore, the size of the pin-jig, the gap between the pin-jigs, and the size of the physical system are fit to the size of the inner car part. Other industries can also implement this system by adjusting these parameters.

By implementing this system, the cost of establishing the manufacturing system can be reduced.

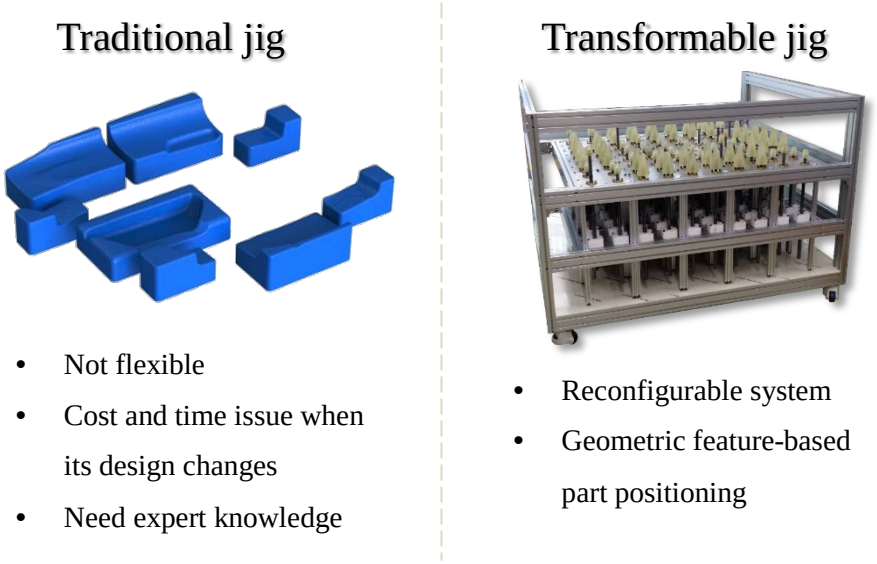

Figure 1. 1 Traditional jig and transformable jig for inner cart part assembly

This thesis consists of six chapters. Chapter 1 introduces the objective of this thesis and provides an overview of the transformable jig. Chapter 2 reviews other researches on the transformable jig system and describes a computer aided design with finite element analysis. Chapter 3 describes the system configuration from the perspective of the testbed. Chapter 4 explains how finite element analysis can help in determining the location of assembly parts and selects the appropriate elements for the analysis of the inner car part assembly. Chapter 5 describes a location decision algorithm with a force estimation model. Finally, Chapter 6 provides the conclusion and states future research.

II. Literature Survey

2.1 Transformable Jig

Flexible Manufacturing System(FMS) was introduced for mass customization and more responsive to change of products. It is suitable for mid-volume and mid-variety production. For implementing these requirements, the initial investment of system is relatively high. Reconfigurable Manufacturing System(RMS) term is used to implement changeable functions and scalable capacity of system. RMS can response to change of product or process rapidly, but it is not fully implemented not yet (ElMaraghy, 2006). To achieve the reconfigurable system, the fixture also should be reconfigurable.

2.1.1 Reconfigurable and flexible fixtures

Traditional jig and fixture have constant shape along with geometry of component holding a single workpiece. Because its lack of flexibility, recent trend of jig and fixture make traditional fixtures have more flexibility. The main implementation methods are (i) Additive Manufacture, (ii) Phase-change Materials, (iii) Modular Fixtures, (iv) Conformable Fixtures(Gameros et al., 2017).

Main reason to use fixture made by addictive manufacturing and phase-change is geometrical degree of freedom. But addictive manufacturing is not proper to mass production and easily wear out during processes(Levy, Schindel, & Kruth, 2003). In the case of phase-change material, main implementation method is thermally-induced state-change method. The heating process to make material melt can also effect to quality of workpice. Other implementation methods are electrorheological and magnetorheological fluid. But their low stiffness in solid state is critical to support against external stress. (Gameros et al., 2017).

Modular fixtures appears faster than other reconfigurable fixtures. Modules are composed of a base-plate, locators, fixtures, and clamps. Types of module can also have different shapes to support various shapes of workpiece. But their position and type should be determined by experts. So many researchers tried to develop automatic modular fixture.

A robot make conformable fixture with high degree of freedom. Li, Xu, Yu, Lou, and Yang (2015) made prototype of fixture with parallel robot to hold metal sheet using 3-2-1 fixture method as presented in Figure 2.2. But there is problem like calibration before fixing and relatively high cost of robot to implement in manufacturing system.

Figure 2. 1 Prototype of fixture with parallel robots adopted from Li et al. (2015)

2.1.2 Pin Tooling

The main implementation methods of conformable fixtures are setting up robots and pin-array. Contrary to fixture with robots, pin-array method commonly reconfigure its shape with actuator. Common types of actuator to implementing pin-array fixture are pneumatic, hydraulic, mechanic and piezoelectric methods. Pneumatic method commonly is applied for fixing large parts. Hydraulic method can hold high pressure, but it is hard to maintain and build a system. Piezoelectric method is extremely accurate but not suitable for moving relatively far distance(Olaiz et al., 2014).

Moreover, there are various attempts to implement pin-array fixtures. Cook, Smith, and Maggs (2008) attempted to actuate pin with seesaw moving base plate and pin locking. Im, Walczyk, Schwarz, and Papazian (2000) tried to actuate pins with lead screw coupled with warm gears. Im et al. (2000) made both flexible mechanical jig and hydraulically actuated jig. In the study, they said each advantage and disadvantage of methods as shown in Table 2.1. Mechanical jig was implemented with different methods, Sequential Set-up(SSU) and Shaft-Driven Leadscrew(SDL). SSU actuates pin by connect leadscrew pin and motor with coupler, changing rotary motion to seesaw motion. SDL actuates pin by connecting shaft and warm gear. Hydraulically Actuated Pin(HA) actuates pin by connecting tube that injecting hydraulic fluid to give pressure.

Table 2. 1 Advantages and disadvantages of each methods adapted from Im et al. (2000)

Method	Advantage	Disadvantage	Figure
Sequential Set-up	Accuracy, repeatability, resolution for pin positioning Less complex than others Self-locking	Long setting time Hard to maintenance No means for detecting engagement of pin	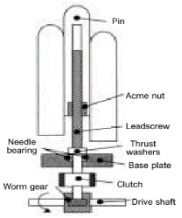
Hydraulically Actuated Pin	Low cost than others One power source Simple control logic Ease to maintenance	Need closed-loop control for driver Checking contact between part and pin High risk for valve-pin interface failure	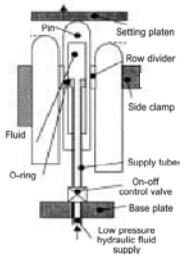
Shaft-Driven Leadscrew	Easy to remove pins Need less space than others Self-locking	Complex than others High cost than others Need large electric power for clutches	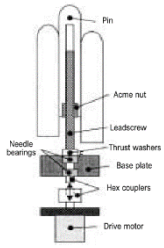

The other example of fixture with hydraulic method is fixture made by Junbai and Kai (2010). They integrated hydraulic method and pneumatic method. Seesaw motion is driven from hydraulic method and pneumatic method make part fixed to pins. They installed hemispheric intake so that pneumatic pressure holds a part while machining like cutting. They decide the location of a part with iterative Finite Element Analysis(FEA) until satisfy some threshold.

2.2 Part stability

Traditional fixture design is based on experience and knowledge of fixture designer. Because cultivating experts is time-consuming process, many researchers tried to make intelligent fixture design system. There are two essential functions and two optional functions to fix a part(Gameros et al., 2017).

i. Essential functions are:

- Location strategy: Determine location and orientation of a part for removing degrees of freedom.

- Clamping strategy: Fix the part while manufacturing processes.

ii. Optional functions are:

- Support strategy: Minimize deformation of the part during the manufacturing processes.
- Tool interaction: Guide and interact with end effector.

Moroni, Petrò, and Polini (2014) dealt with locator location problem for reducing volumetric error and defect. There is also reconfigurable fixture system with vision sensors. This is called Affordable Reconfigurable Tooling system that calibrate with vision system. Vision sensors recognize the posture and position of parallel robots so that calibration. However, this system does not calibrate automatically, but manually. And only concerned about the accuracy of part location positioning, but stress and deflection of part(Jonsson & Ossbahr, 2010). Follmer, Leithinger, Olwal, Hogge, and Ishii (2013) make an interactive system with depth camera. The camera compute a distance between a part and a plane. Their system can track the part in real-time. But the resolution in 2-dimensional plane is 2mm and 10mm in 3-dimentional space. Therefore, it is not suitable for manufacturing system.

For designing intelligent fixture, below conditions are necessary.

- Automated designing
- Practical knowledge of fixture design
- Use of proven structure
- Parametric design along with required usage
- Verification capability

Requirements can be achieved with CAD, but knowledge of expert cannot be easily approached. Therefore, Computer Aided Fixture Design(CAFD) is necessary. And since the 1990s, CAFD have been actively researched to achieve reconfigurable fixture system. Implementation methods of CAFD are case based reasoning, genetic algorithm, and CAD based collision detection, etc. And finite element method(FEM) is typical method for analyzing stress and deflection of part(Rong, Huang, H, & Hou, 2005; Wang, Rong, Li, & Shaun, 2010). Basic process of CAFD is presented as Figure 2.1.

One of the example is the list up processes of cutting, such as making hole, and setup the tools according to those features to 3D CAD of workpiece(Attila, Stampfer, & Imre, 2013). The study to reduce positioning error in setting up modular fixture tried to control their position with sensors and actuators. And also by integrate cad model and real machine, control predict a process with parameters(Olaiz et al., 2014).

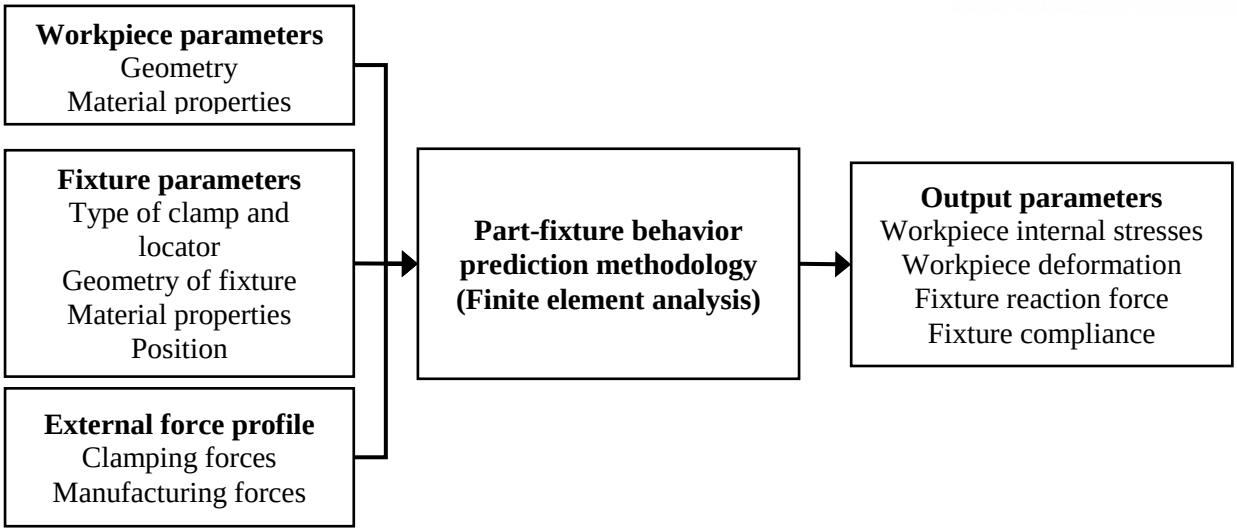

Figure 2. 2 The basic elements of the fixture design process and typical FEM based fixture design solution analysis framework adopted from Wang et al. (2010)

Many researchers presented various finite element and analytic solutions in the point of view of curved beam. One of the analytic solution for mixed curved-beam finite elements was developed based on form of the nonlinear deep-arch theory. According to the fundamental equations of nonlinear deep arch theory, the local curvature of the arch is related to bending moment and normal force(NOOR, GREENE, & HARTLEY, 1977). The functional equation is as follows:

$$\Pi(\mathrm{N},\mathrm{Q},\mathrm{M},\mathrm{u},\mathrm{w},\phi) = V - U^c - W,$$

$$\mathrm{V} = \int \left[\left\{\partial_s u + kw + \frac{1}{2}(ku - \partial_s w)^2\right\}N + (\partial_s \phi)\mathrm{M} + (-\mathrm{ku} + \partial_s w + \phi)\mathrm{Q}\right] ds,$$

$$\mathrm{U^c} = \frac{1}{2}\int [aN^2 + 2bNM + gM^2 + a_s Q^2] ds,$$

$$\mathrm{W} = \int (P_s u + pw) ds + \sum\left(\tilde{N}u + \tilde{M}\phi + \tilde{Q}w\right) + \sum[N(-\tilde{u} + u) + M\left(-\tilde{\phi} + \phi\right) + Q(-\tilde{w} + w)],$$

$$\mathrm{u} = \eta\psi_1, w = \eta\psi_2, \phi = \eta\psi_3,$$

where V is potential energy associated to the applied forces, $\mathrm{U^c}$ is complementary energy of the arch, W is work done by external forces, k is local curvature of the arch, M is bending moment, N is normal force, η is shape function, ψ is nodal displacement parameters, a, b, g and $\mathrm{a_s}$ are arch compliances, $\mathrm{P_s}$ and p are external load components.

Another researcher analyzed curvature- and displacement-based finite element solution with flexible four-bar mechanisms. Their formulation is based on the two-element discretization having a linear function of the curvature for each link(Kuo & Cleghorn, 2010). They apply the Euler-Lagrange equations, which are related to curvature.

Bin and Wanji (2010) proposed analytic solution, considering effects of both elastic deformation and plastic deformation. And the solution implicitly gives relationship between the moment and the curvature. They simulated pure bending part that is composed of both plastic and elastic materials as Fig 2.3.

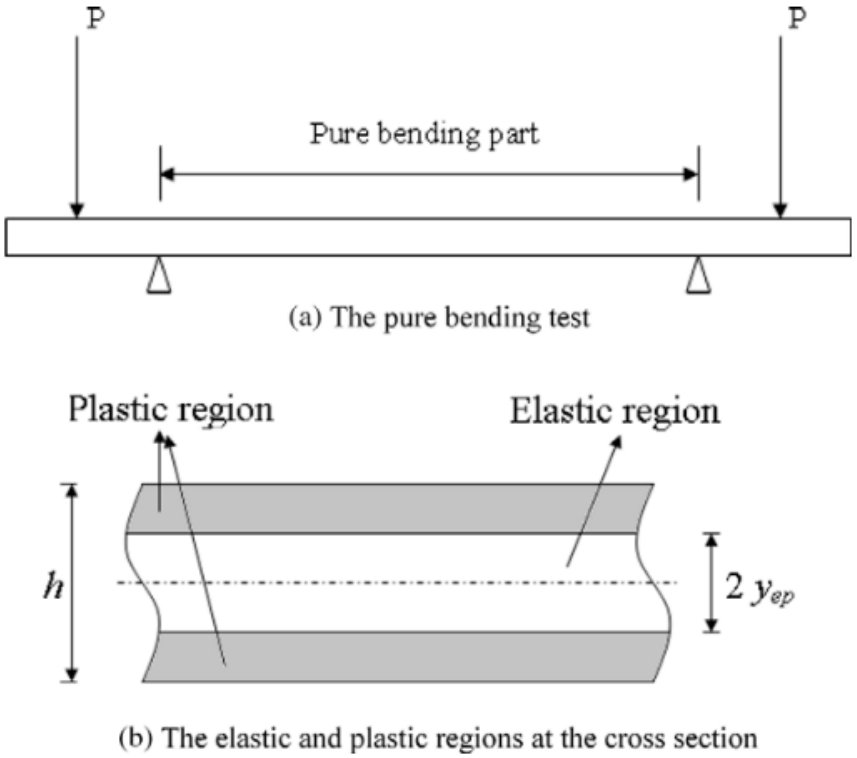

Figure 2. 3 The schematic diagram of pure bending test with elasto-plastic deformation derived from Bin and Wanji (2010)

Zhang et al. (2011) compared the Young-Laplace law and finite element method, applying both to ventricular wall stress problem. The derivation of the Young-Laplace law is as follows:

$$\sigma[\pi(\mathrm{r}+\mathrm{h})^2-\pi\mathrm{r}^2]=P\pi r^2$$

where P is intracavitary pressure, r is the endocardial radius of curvature, and h is the wall thickness. And they modified the Young-Laplace law as follows:

$$\sigma=\frac{\mathrm{pr}}{2h}$$

, assuming h << r. Above methods are tried to draw an exact stress, comparing solution of finite element method. But their methods did not draw exact stress.

Siebenaler and Melkote (2006) tried to find more accurate deformation of workpiece using friction parameter and mesh density of finite element analysis. The used model consist of contact mechanics, 10-node tetrahedral element and friction between fixture and workpiece. They compare the result of

FEA and experimental result with eddy current proximity sensors. The hardware consist of six locators and two clamps as shown fig 2.5. They examine the deformation of steel rectangular shell. The error rate of reaction force and deformation in specific area was within 5%.

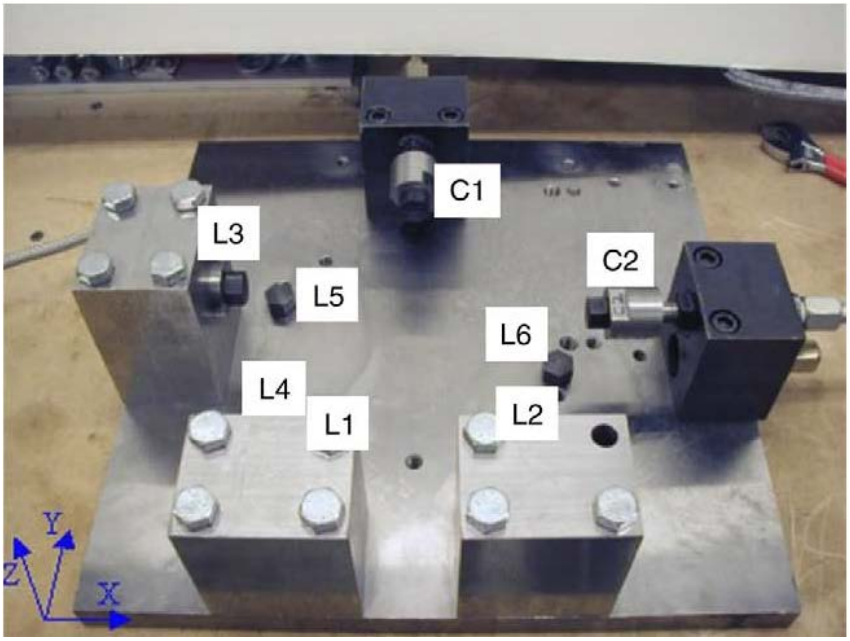

Figure 2. 4 Experimental setup of fixture

Alternatively, I used 3D scanner for detect the larger deformation of whole workpiece. And I will compare results among different elements.

III. A Transformable Jig System

3.1 System configuration

The purpose of the transformable jig system is implementing rapidly reconfigurable jig with user-friendly interface. The transformable jig system consists of a software and a hardware. The software controls the shape of transformable jig. The input of transformable jig system is 3D CAD model of a part.

3.2.1 Transformable Pin-Jig

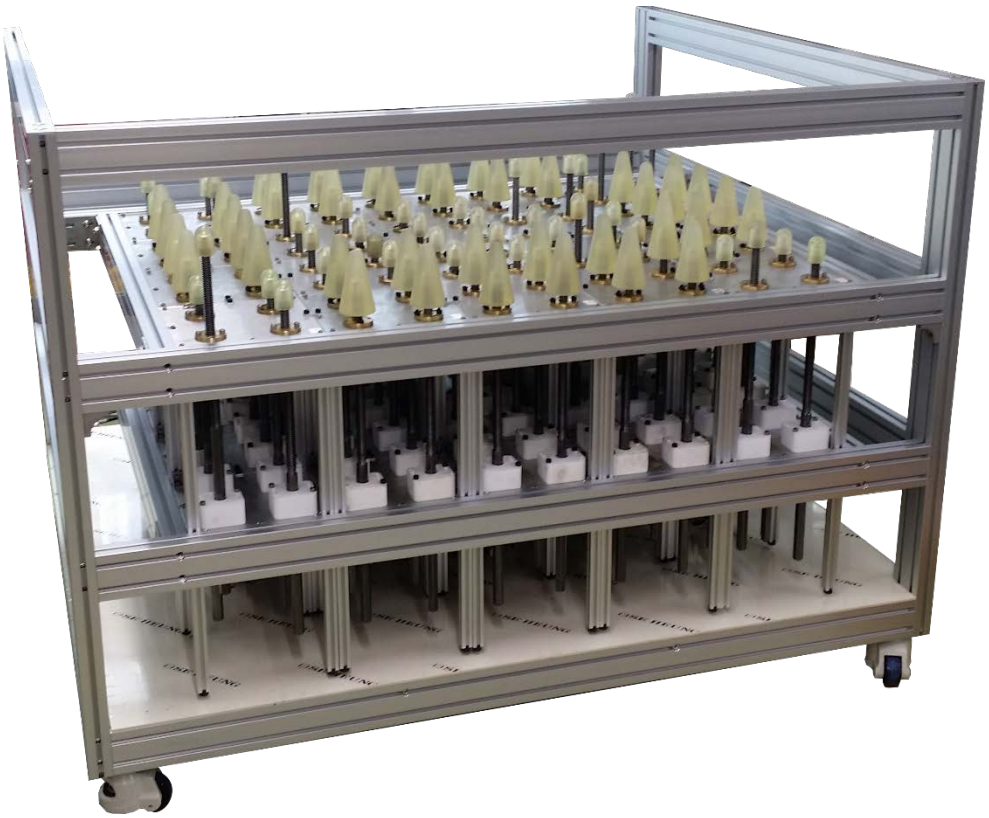

Figure 3. 1 Transformable Pin-Jig Testbed

The hardware of transformable pin-jig system consists of n by m modules that contains four pin-jigs as Figure 3. 1. Current modules are arranged in the transformable pin-jig system along with 5 by 4 modules. The whole frame made by aluminum supports modules and other accessories such as motor drivers and computer. These modularization of system can support less laborious maintenance. Each motor drivers are connected with each other by Ethernet cable using daisy chain. As a result computer need only one Ethernet port.

Table 3. 1 Specification of the system

Component	Specification
Frame	Allowable part size: 1120X880mm^2 Body: 80X80 aluminum Module: 40X40 aluminum
DC Servo Motor	Closed loop control Resolusion: 16,000 RPM: 3000
Motor driver	Torque: 0.2N·m Ethernet Daisy chain connect
Pin-jig screw	Steel Pitch: 3mm Radius: 6.5mm
Pin-jig cap	Polyurethan shape : hemisphere, cone
Controller OS	PC with windows 10
Caster	Allowable load: 784daN
Gear	Steel spur gear

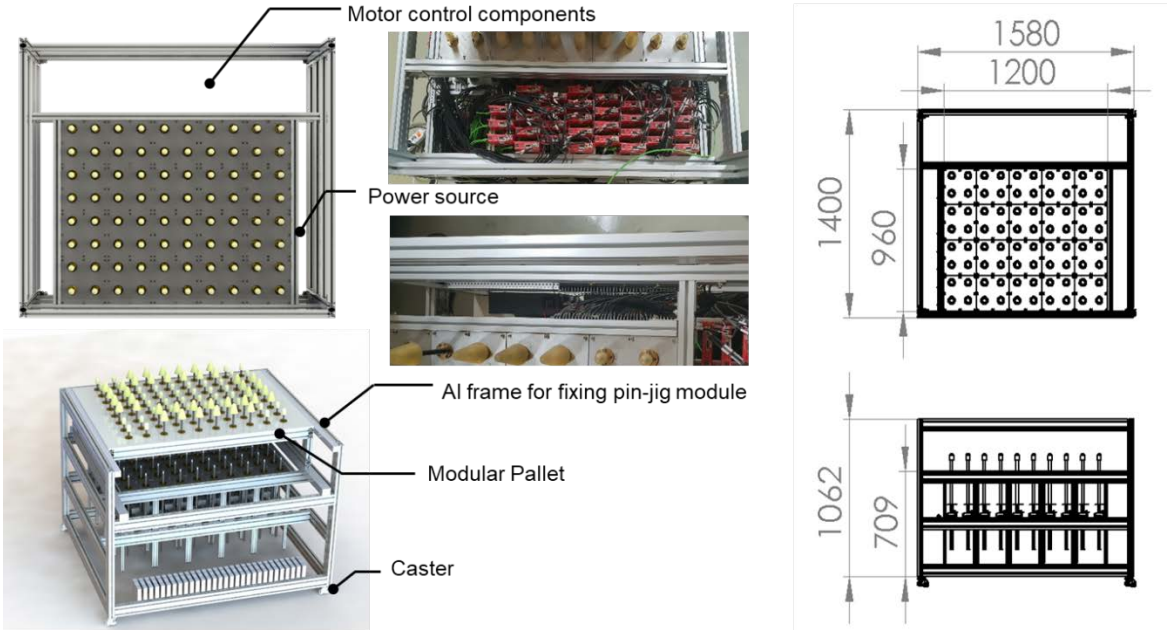

Figure 3. 2 Hardware configuration of transformable pin-jig system

A module consists of aluminum frame, four pins and motors, and gearboxes as Figure 3. 6. On the top of each pin, polyurethan cylinder that has round-cut tip is assembled, preventing flaw in a process like scratch on the part. A pin is divided into two body, screw and hexagon rod. Four rubber feet support whole body at the bottom of the columns of frame, reducing vibration through body that can affect accuracy of motor rotation. Each motor is connected to each motor driver by interference-resistant wires. In addition, each motor driver communicates with a computer that has 3D Pin-Jig Shape Transformer connected with Ethernet cable. Motor driver transfers motor states such as current position, velocity and position error. Intervals between pins are both 120mm.

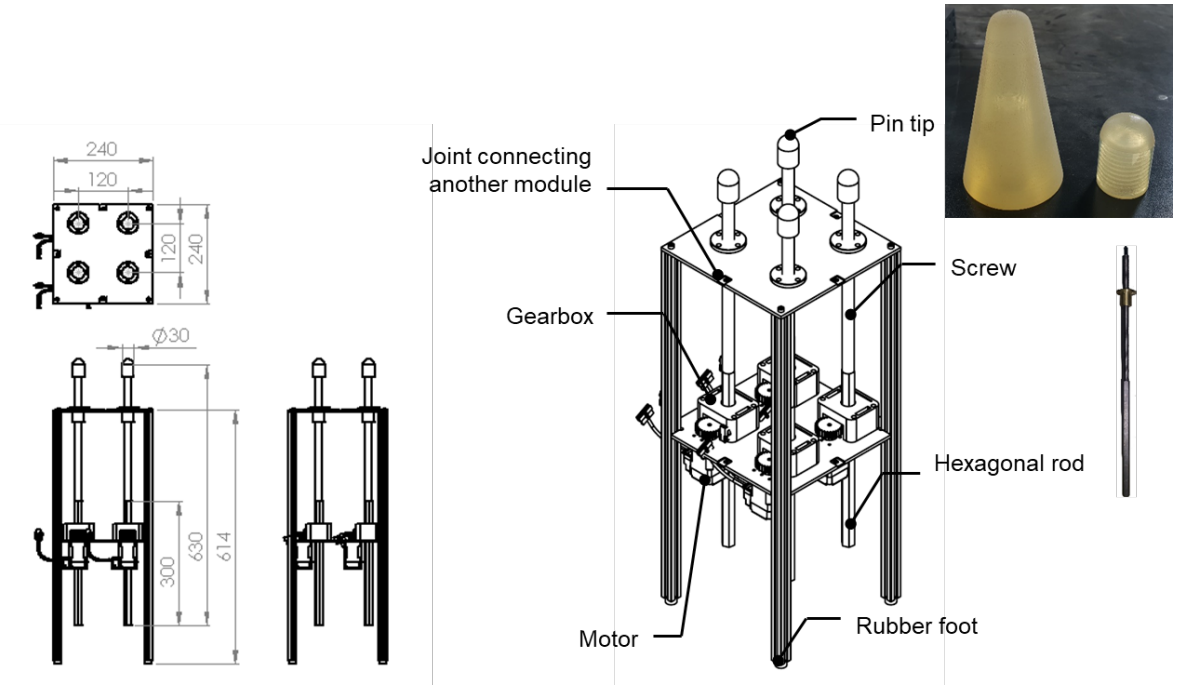

Figure 3. 3 A module of transformable pin-jig system

A servo motor with gear transfer power to a pin-jig as Figure 3. 6. The pin-jig is screw connected on the top of hexagon rod. The gear on the motor make a gear rotate, which has hexagon hole at the center and engage with hexagon rod of pin-jig. The screw of pin-jig engages with a nut. As gear wit hexagon hole rotates, pin-jig rotates and screw of pin-jig moves forward and backward according to direction of rotation. As result, the servo motor can adjust a height of pin-jig.

Figure 3. 4 Joint (left), joining location (middle) and connecting two module (right)

Figure 3. 5 Servo motor (left) and its Driver (right)

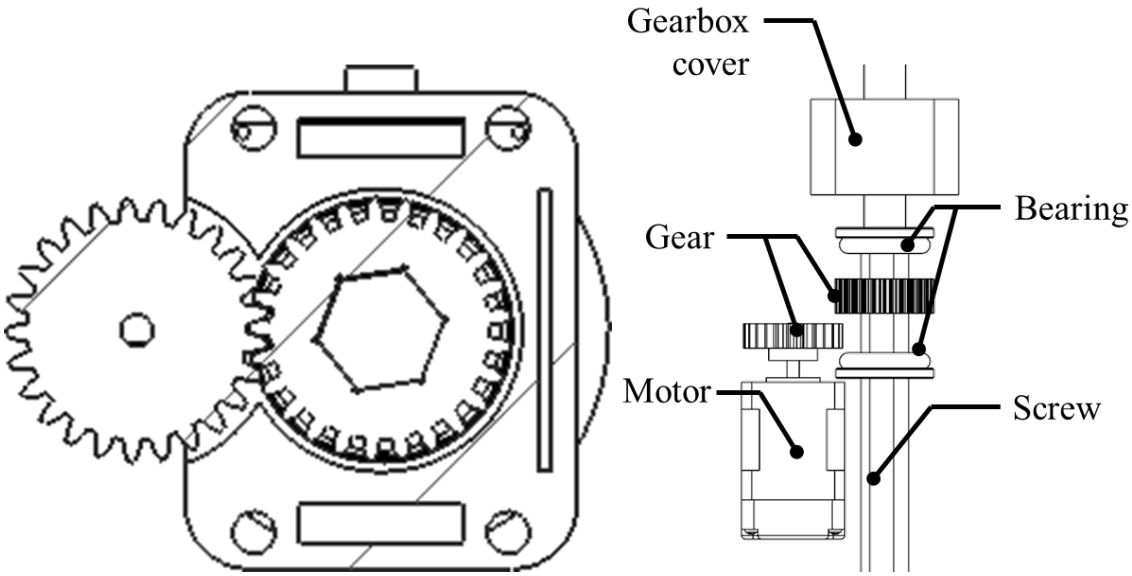

Figure 3. 6 Gears and pin-jig shapes for power transformation from motor to pin-jig

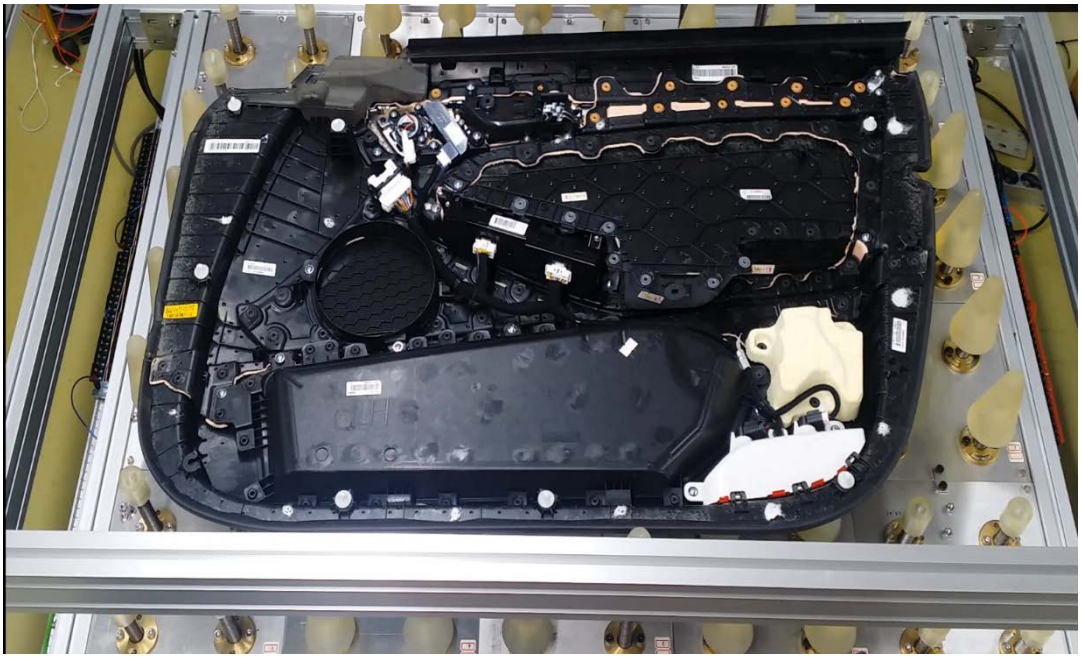

Figure 3. 7 Example of supporting a part (Doortrim – Seoyeon Iwa)

3.2.2 3D Pin-Jig Shape Transformer

Target environment of software is Window 8.1 and development language is C++ with Qt4 software development kit. Representation of 3D CAD model on the screen is support by open-source library Visualization ToolKit (VTK).

A 3D Pin-Jig Shape Transformer reads 3D CAD model of a part and calculates the heights of each pin-jigs. The type of 3D CAD model is Standard Triangulated Language (STL). STL is most common neutral format for represent CAD in CAM system (Pham & Dimov, 2001). In addition, STL presents 3D CAD with polyhedral surfaces. The polyhedral surface approximates linearly to the underlying surface, and its data exchange and geometric computation is simpler and more robust than that of parametric surface(Xu, Sun, & Wang, 2012). For ease of computation with VTK, STL is converted to Visualization Toolkit Polygon (VTP).

Table 3. 2 Software configuration

Type	Component
Target operating system	Windows 8.1
SDK	Qt 5.8
Development language	C++
Library	Visualization ToolKit (VTK) 7.1.0

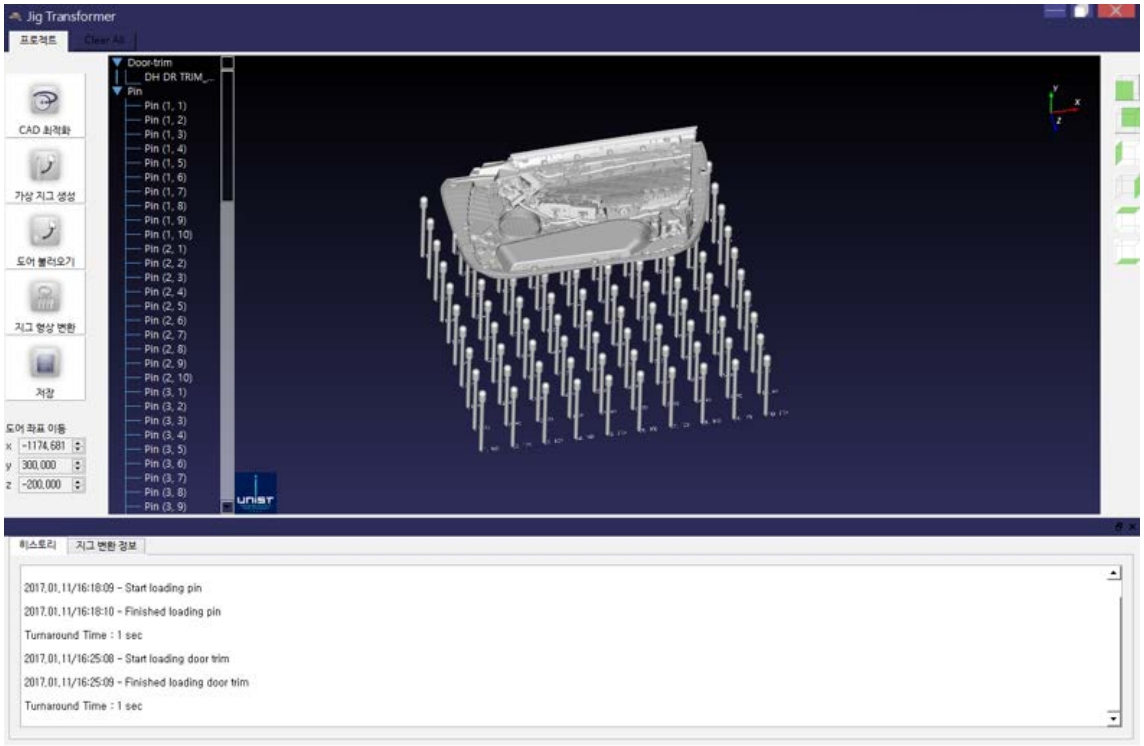

Figure 3. 8 Initial setup of 3D Pin-Jig Shape Transformer

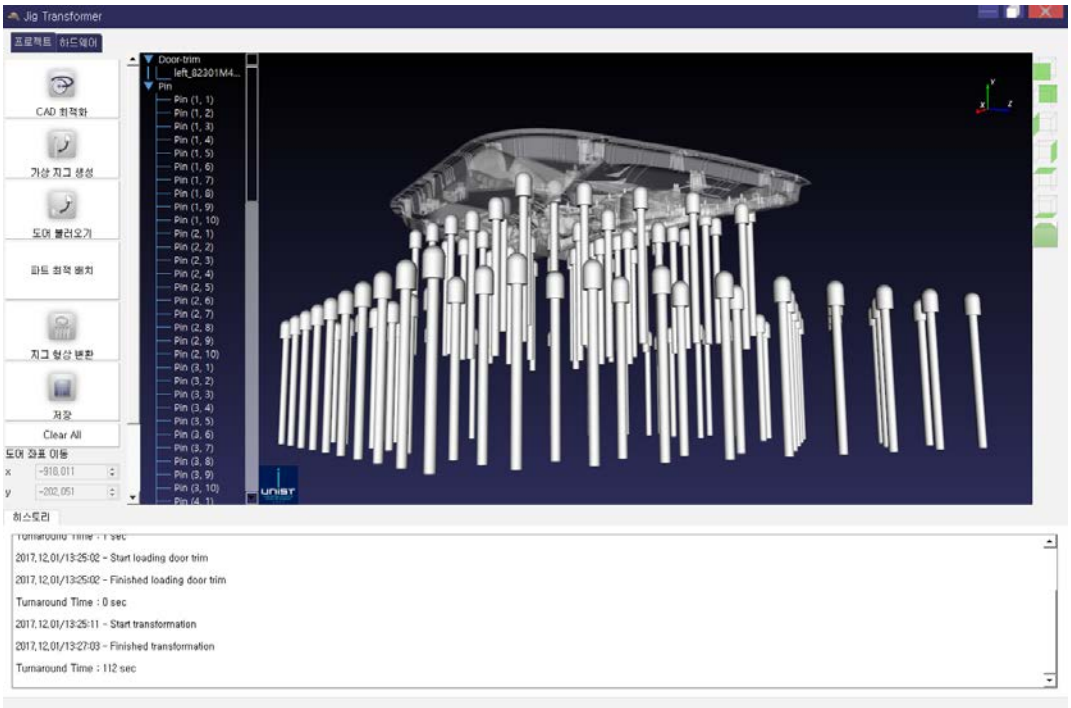

Figure 3. 9 Pin-jig stroke calculation

Functions

In the 3D pin-jig shape transformer, there are several functions to calculate strokes of pin-jigs. Followings are detail of functions:

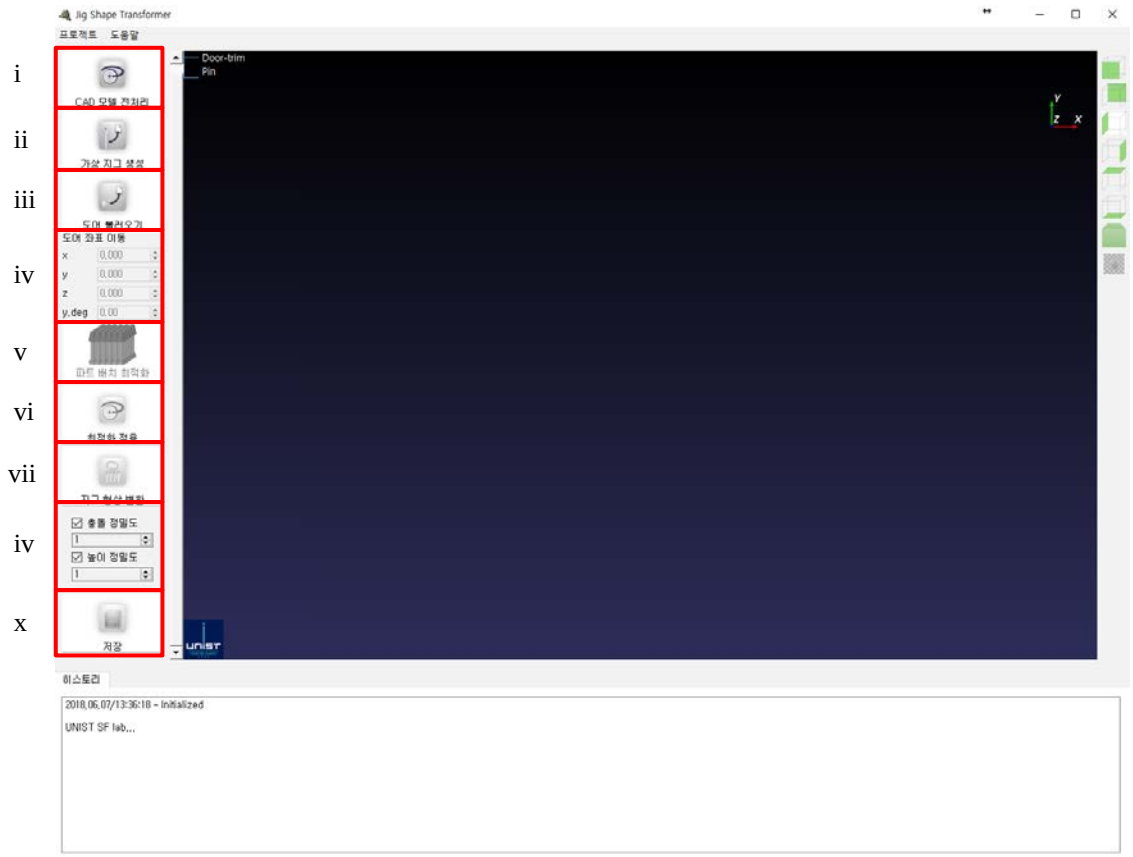

Figure 3. 10 Functions of 3D Pin-Jig Shape Transformer

i. Preprocess of CAD model

From STL file, remove unnecessary information such as no-thickness surface or line.

ii. Setup virtual pin-jigs

Import the 3D CAD of a pin-jig. Determine the number of pin-jigs.

iii. Load a part

Import the 3D CAD of a part. Determine which surface is bottom of product.

iv. Setup coordinates of the part on pin-jigs

It can move along 3-axis and tilt against y-axis.

v. Open optimal part positioning program

It is related to other research about optimal part positioning on pin-jigs.

vi. Optimal assembly part positioning using geometric feature-based estimation model

Using 3D CAD of the part and the setup information, it finds optimal coordinates of the part.

vii. Calculate strokes of pin-jigs

Get each strokes of pin-jigs. It also visually shows the result of operation as shown Figure 3. 9.

iv. Accuracy rate of stroke calculation

Determine how much precision is required when calculate strokes of pin-jigs. It has two types of accuracy. One is interference accuracy and the other one is resolution of moving a pin-jig.

x. Save the result

The result contains strokes of pin-jigs. It will transfer the number of rotation of each motors using this result to transformable pin-jigs.

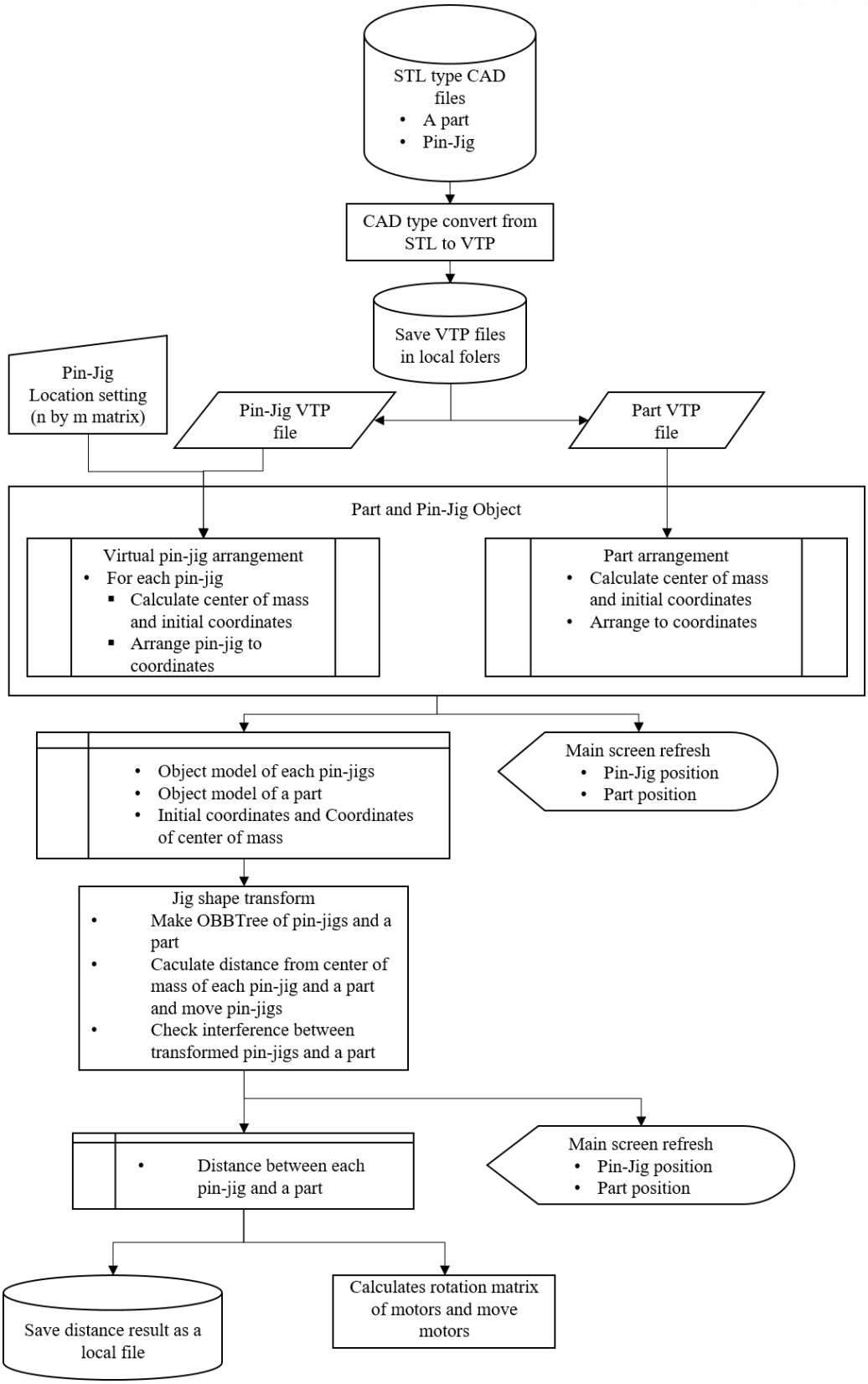

Figure 3. 11 Process flow chart of 3D Pin-Jig Shape Transformer

Following statements are detail of processes:

Preprocess

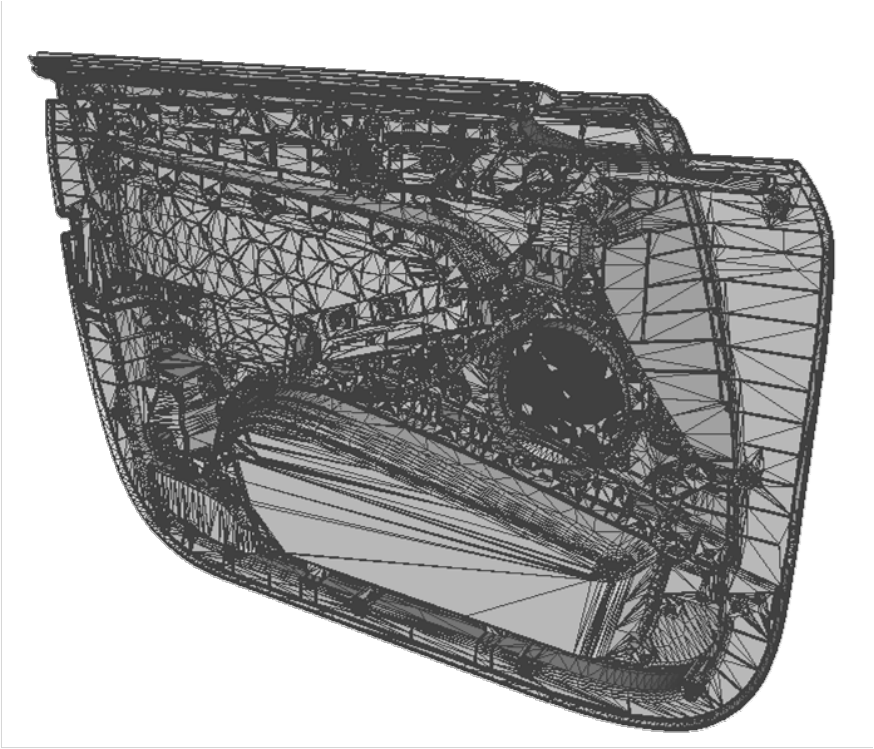

Figure 3. 12 Example of triangular mesh of inner car door trim

For a computation of heights of pin-jigs or checking interference with function in VTK, STL files of a part and pin-jig should be converted to VTP. After converting, load pin-jig and a part file, calculating center of mass and save coordinates in the local memory with center of mass. Pin-jigs is arranged in an n by m matrix, where n is the number of pin-jigs along with x-coordinates and m is the number of pin-jigs along with z-coordinates.

Before calculation of distance between pin-jigs and a part, clip a part with several rectangular parallelepipeds that cover area of each pin-jigs for select effective computation of interference. The clipping process copies triangular meshes in the area to memory, and create OBBTree only with triangular meshes in the area. If one point of the triangular mesh is outside the region, the triangular mesh is not included in the clipping. Therefore, if the center of mass of the triangular mesh is in the region, the area included the mesh forcibly. In addition, the size of area can be adjusted so that the regions slightly overlap each other for reducing missing meshes. Basically, the size of area depends on the size of the pin and heuristic decisions.

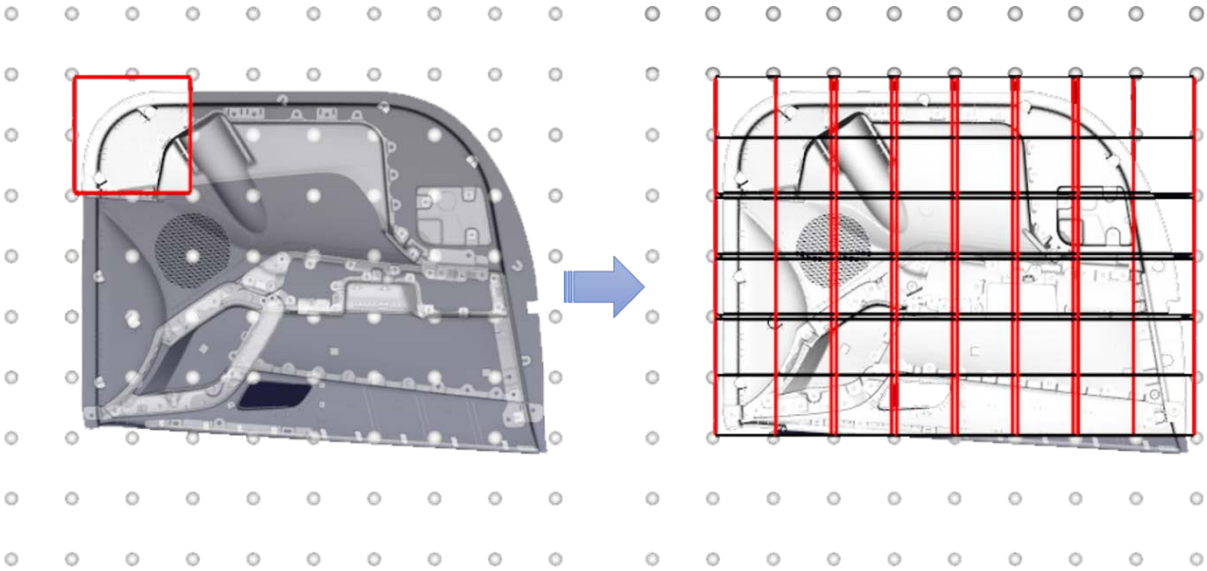

Figure 3. 13 Clipping a part according to each pin-jig

Stroke calculation of pin-jigs

For calculation of distance from each pin-jig and isosurface of a part, draw a line from center of pin-jig along with y-coordinates through a part. The distance is calculated by get distance between an interference point that is on the top of pin-jig surface and a lowest interference point of the part.

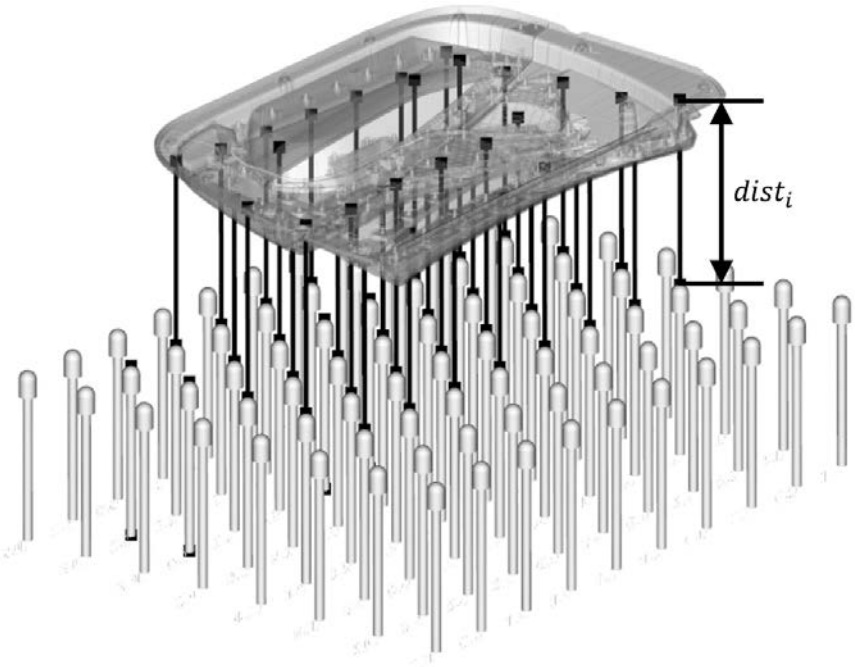

Figure 3. 14 Distance between an interference point that is on the top of pin-jig surface and a lowest interference point of a part

However, transforming a pin-jig according to the distance may occur interference between the pin-jig and a part as presented in Figure 3.5, not considering the shape of the part and a pin-jig. These interference can be easily solved by transfer each pin-jig downward iteratively until the number of points and lines satisfy an appropriate threshold according to volume of the part and a pin-jig. The greater volume the part and a pin-jig have, the higher value threshold become.

After calculation over, save the result on the local storage for transmitting value to each driver of each motor.

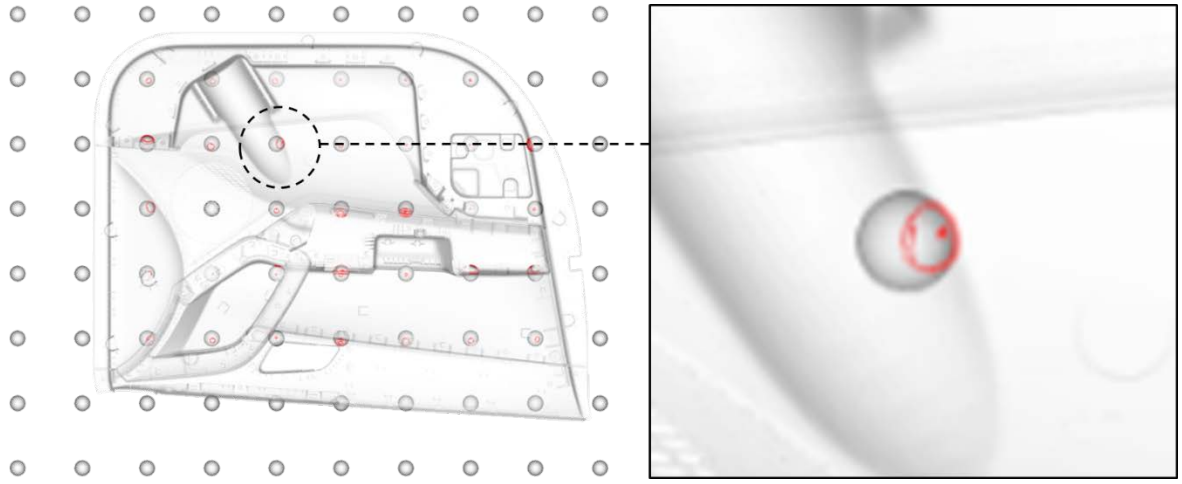

Figure 3. 15 Interference (red line) between a part and each pin-jig

IV. Finite Element Analysis for Part Positioning on Pin-Jigs

In this chapter, I will describe some elements of finite element analysis and apply it to the preceding problem. The door trim shown above can be interpreted as a plate element, shell element or a solid 3D element. Therefore, I will summarize the problem so that it can be interpreted as a plate element or a 3D element.

A typical process of finite element analysis(FEA) is as follows .

i. Decide an element type of part and discretize by the element

ii. Determine a displacement function of the element in a local coordinate

iii. Define a strain/displacement and stress/strain relationships

iv. Derive the element stiffness matrix and equations

A. Direct equilibrium method
   - Derive a relationship between nodal force and nodal displacement and a stiffness matrix. It use the force equilibrium condition for the element. It is often used for 1D elements.

B. Work or energy methods
   - This method is easier than the previous method when derive a stiffness matrix and an equation of 2D and 3D elements. Types of methods include the principle of virtual work, the principle of minimum potential energy, and Castigliano's theorem. The principle of minimum potential energy, Castigliano's theorem method, is applicable only to elastic materials.

C. Weighted residual methods
   - Candidate of method is Galerkin’s method. A same result is obtained when the energy method is applicable. It is useful when potential energy cannot be used.

D. Get an equation using a previous method.

$$\begin{Bmatrix} f_1 \\ f_2 \\ \vdots \\ f_n \end{Bmatrix} = \begin{bmatrix} k_{11}k_{12}\cdots k_{1n} \\ k_{12}k_{22}\cdots k_{2n} \\ \vdots \\ k_{n1}k_{n2}\cdots k_{nn} \end{bmatrix} \begin{Bmatrix} d_1 \\ d_2 \\ \vdots \\ d_n \end{Bmatrix}, \{f\} = [k]\{d\}$$

Where *f* is elemental nodal vector, *k* is element stiffness matrix, *d* is unknown element nodal degree of freedom or generalized displacement(actual displacement, slopes, curvature, etc.)

v. The element equations are combined to form the global (total) equation, and the boundary conditions are determined.

$$\{F\} = [K]\{d\}$$

A. *K* is a singular matrix because its determinant is zero. To solve this problem, apply a boundary condition. Boundary condition means fixing a certain elements in body.

vi. The above global equation can be solved using the gauss's elimination method or the iterative method (Gauss-Seidel method) to obtain *d*.

In this finite element analysis, I consider a plate fixed with four pin-jigs. Because whole product on the transformable pin-jigs can be divided into many plates. The standard of boundary cutting is contact point between a part and four pin-jigs. These can be represented as four boundary points in finite element analysis. The type of finite element can be a plate element or 3D solid element. By considering results of each finite element analysis, it can substitute the result on a whole part comparatively.

For the integration of 3D pin-jig shape transformer without commercial program, I implement the finite element analysis program with MATLAB.

4.1 Plate bending element model

A plate element commonly used to analyze pressure vessels, chimneystacks and automobile parts. When a plate is curved, then it becomes a shell element (Logan, 2016). I will consider the Kirchhoff assumptions for establish basic behavior of an element. I will compare a result of finite element analysis with a triangular element to a result of rectangular shell element. The triangular element, also called constant-strain triangle(CST), is on 2-dimensional space. I choose the CST because STL also consists of triangular meshes.

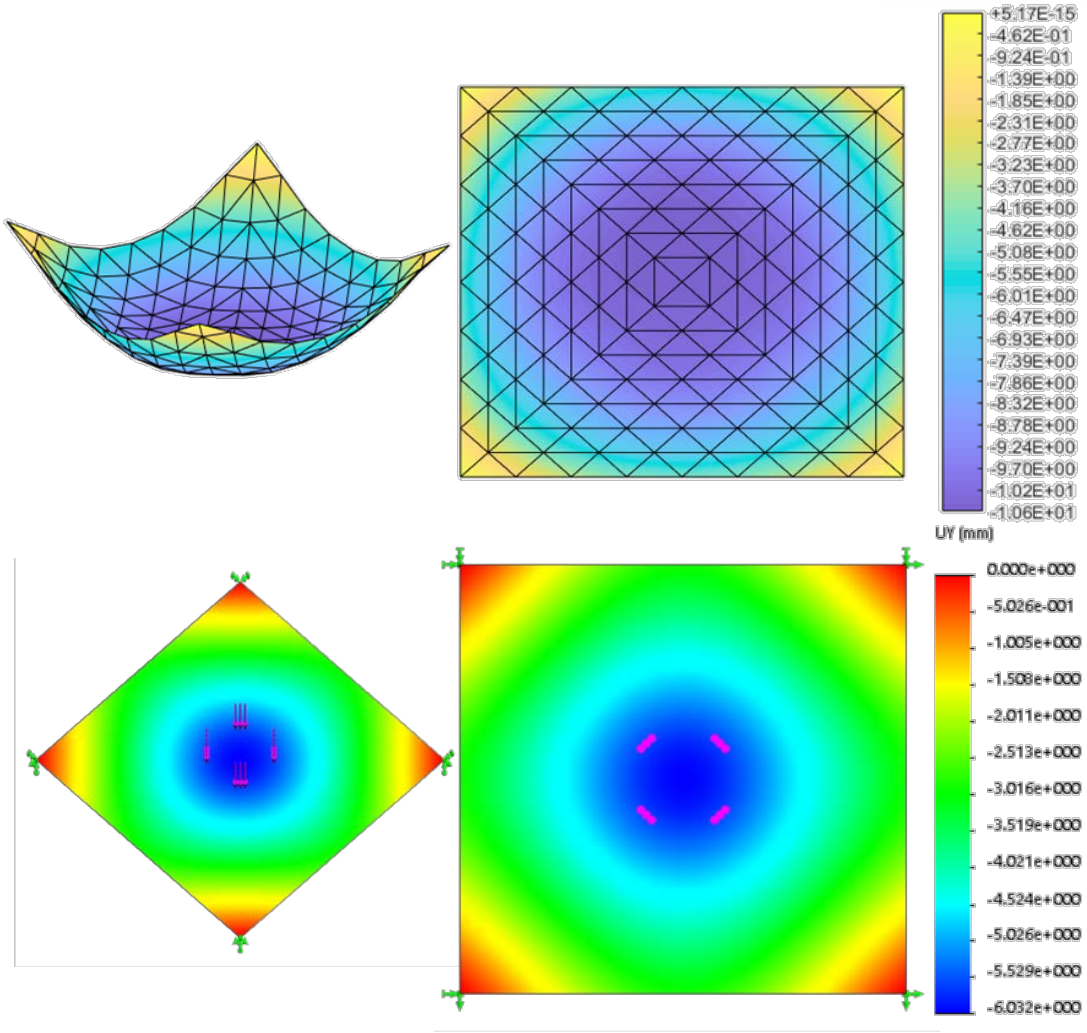

Figure 4. 1 Result of Kirchhoff plate theory (top) and result of commercial shell element FEM (bottom)

4.2 3D element model with large deformation

The 3D element commonly is classified into two types. One is the tetrahedral element and the other one is the hexahedral element. I used the tetrahedral element for the finite element analysis. The figure 4. 2 is the comparison of results between finite element analysis with tetrahedral element and that of commercial.

In the process of finite element analysis, I apply the large deformation theory. The large deformation theory is the total Lagrangian method with Newton-Raphson iteration solve.

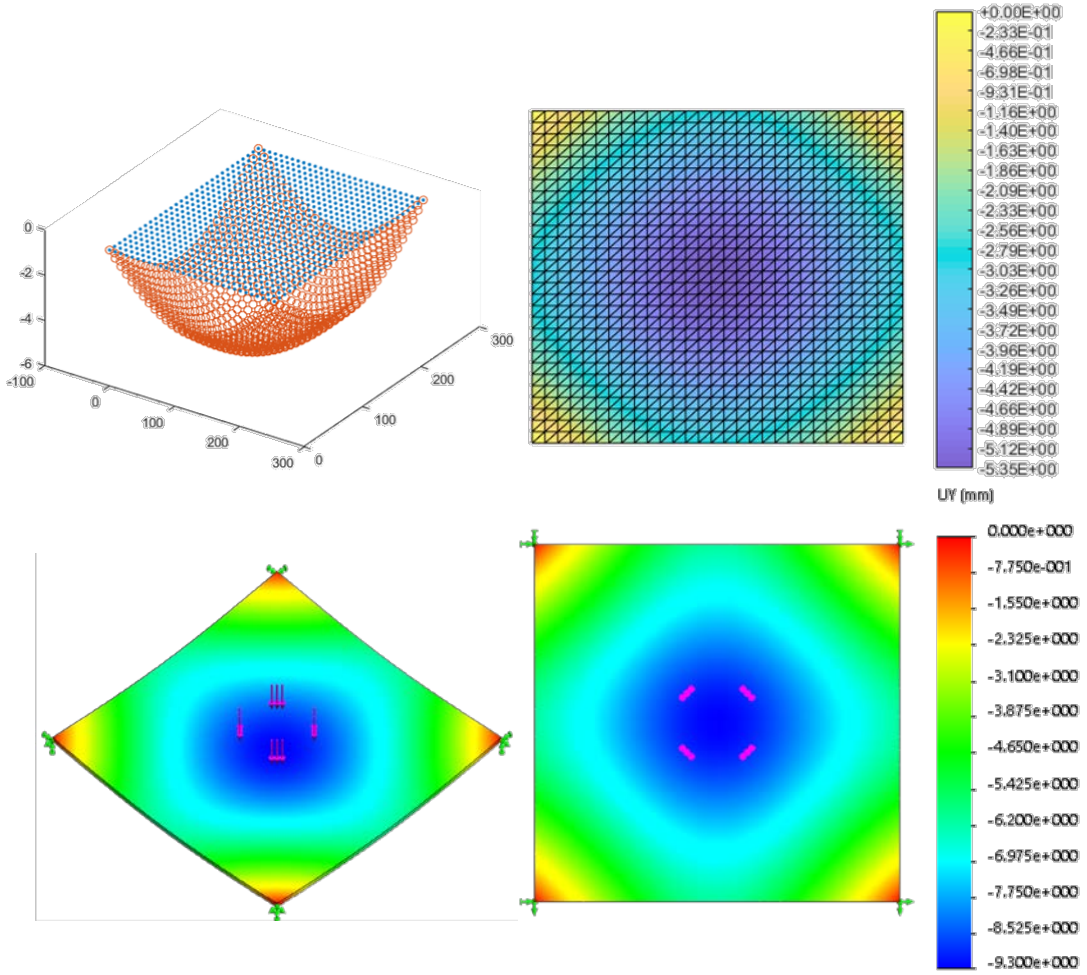

Figure 4. 2 Result of tetrahedral element (top) and result of commercial 3D element FEM (bottom)

The table 4. 1 shows that there are some difference between largest deformation results. I implement finite element methods with plate element and 3d solid element, and compare the result of pressing a divided part to result of commercial software. There are some errors in the amount of deformation, but its trend of result shows similarity. Mesh quality, base theory or a solver affects the result of deformation.

Table 4. 1 Largest deformation of each finite element method

	Plate element	Shell element (commercial S/W)	3D solid element	3D solid element (commercial S/W)
Largest Deformation(mm)	10.66	6.032	5.35	9.300

4.3 Finite element analysis for extract estimation factors

Extraction of estimation factors from a simple plate

With above two methods, I apply those to assembly problems. The plate or 3D solid model can be considered as the part of car inner door modules. The variable of experiment is a gap between boundary and external force. The external force means the assembly joining pressure. The location of external forces are determined as shown Figure 4. 3.

As shown Table 4. 2, the gap between boundary and external force is related to each other. To prevent the degradation of assembly quality, the deformation during the process must be minimized. For minimizing the deformation of the plate, the gap between boundary and external force should be shorter.

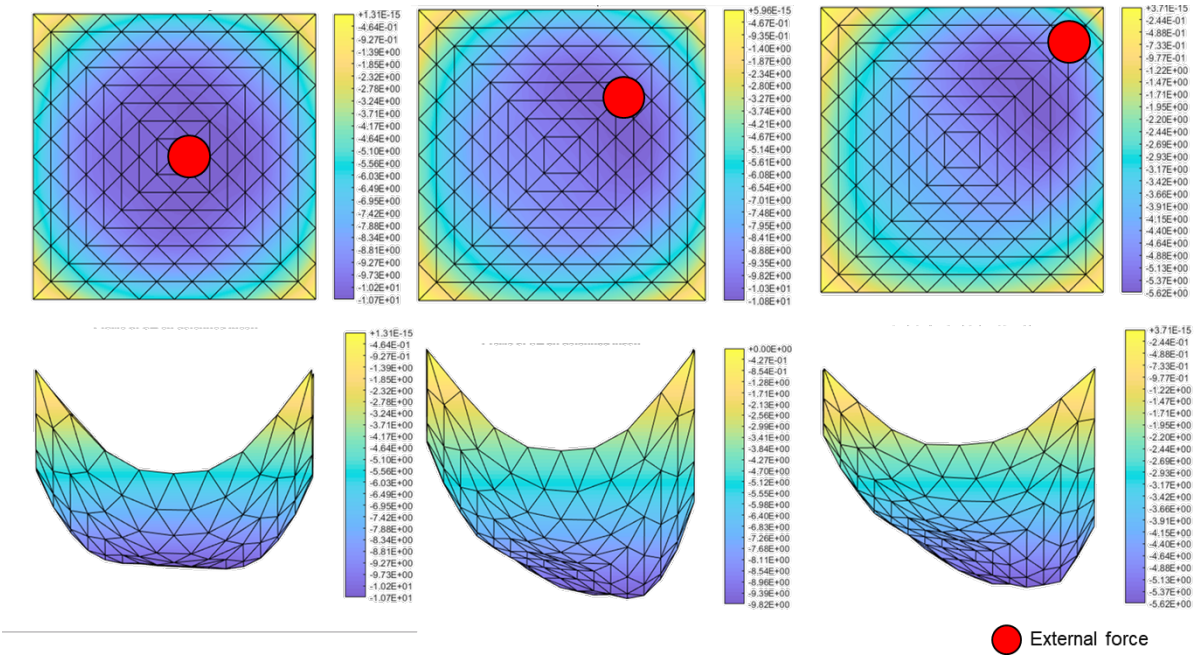

Figure 4. 3 Location of external forces on a plate

Table 4. 2 Result of finite element analysis

Gap between boundary and external force(N)	Plate element largest deformation(mm)	3D element largest deformation(mm)
0.49	10.66	5.35
0.25	9.81	4.33
0.07	5.61	3.73

In addition, I conduct an experiment to examine investigate the effects of plate shape on the results of finite element analysis. There are concave, convex, and flat types in the form of plates. In the experiment, concave and convex plate has same curvature. Each experiment has five different support location and each support location has four support points. Moreover, there are nine different external load location on each plate. Therefore, there are forty-five experiments on each shapes. Each experiments give same amount of power on the surface. The used finite element is 3D solid element. The plate is composed of tetrahedron mesh. Amount of external load and the deformation assume that the experiment is under the linear elastic deformation.

Each result shows the deformation within the area influenced by external load, because I interest area for assembly quality is within assembly area that is area influenced by external load.

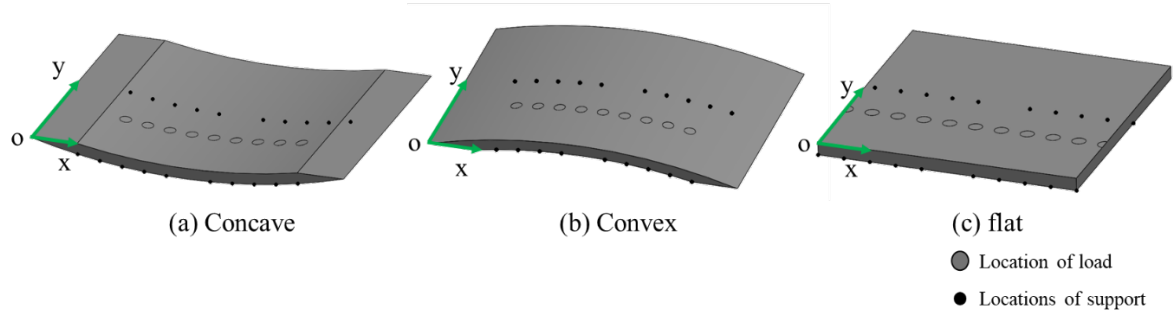

Figure 4. 4 Design of an experiment

The average deformation is the least in the convex plate, then in the concave plate, and the flat plate was the most deformed. Average deformations are 1.25E-2, 9.92E-3, and 1.38E-2 in the order of the figure 4. 4. They also shows that almost every deformation at center of support points is largest against other that of different distance from points.

Table 4. 3 Deformation of the experiment on concave surface within location of load

e \ f'	0	20	40	60	80
20	1.38E-02	9.93E-03	1.06E-02	1.02E-02	1.02E-02
40	1.42E-02	1.32E-02	1.29E-02	1.27E-02	1.30E-02
60	1.46E-02	1.40E-02	1.38E-02	1.40E-02	1.46E-02
80	1.30E-02	1.27E-02	1.28E-02	1.31E-02	1.42E-02
100	1.02E-02	1.03E-02	1.06E-02	1.13E-02	1.37E-02

f': distance between the origin ‘o’ and the closest jig points to ‘o’,
e: distance between the center of external load ‘c’ and the closest jig point to ‘c’

Table 4. 4 Deformation of the experiment on convex surface within location of load

e \ f'	0	20	40	60	80
20	1.21E-02	1.03E-02	9.50E-03	9.21E-03	9.16E-03
40	1.16E-02	1.07E-02	1.03E-02	1.03E-02	1.05E-02
60	8.33E-03	1.09E-02	1.08E-02	1.10E-02	1.15E-02
80	6.00E-03	1.02E-02	1.03E-02	1.07E-02	1.16E-02
100	9.15E-03	2.11E-03	9.50E-03	1.03E-02	1.21E-02

f': distance between the origin ‘o’ and the closest jig points to ‘o’,
e: distance between the center of external load ‘c’ and the closest jig point to ‘c’

Table 4. 5 Deformation of the experiment on flat surface within location of load

e \ f'	0	20	40	60	80
20	1.93E-02	1.27E-02	1.15E-02	1.10E-02	1.10E-02
40	1.57E-02	1.33E-02	1.28E-02	1.27E-02	1.32E-02
60	1.68E-02	1.53E-02	1.51E-02	1.54E-02	1.48E-02
80	1.32E-02	1.28E-02	1.28E-02	1.32E-02	1.58E-02
100	1.10E-02	1.11E-02	1.14E-02	1.27E-02	1.94E-02

f': distance between the origin ‘o’ and the closest jig points to ‘o’,
e: distance between the center of external load ‘c’ and the closest jig point to ‘c’

Extraction of estimation factors from 3D solids with mixed shapes

Finite element analysis was performed on mixed shapes to extract various factors from plate. Because a plate element cannot has limited representation, I used the 3D solid elements for representing various shapes.

This experiment was carried out by classifying the shapes in the car inner door module. The car inner door module consists of the following four shapes as shown figure 4. 4.

i. Curved/tilted surfaces: surfaces with different radius of curvature or tilt angle

ii. Plate surfaces: flat surfaces connected with curved surface

iii. Stepped-shape surfaces: surfaces that has L-shaped between two surfaces

iv. C-shaped surface: surfaces that has a pillar between two surfaces

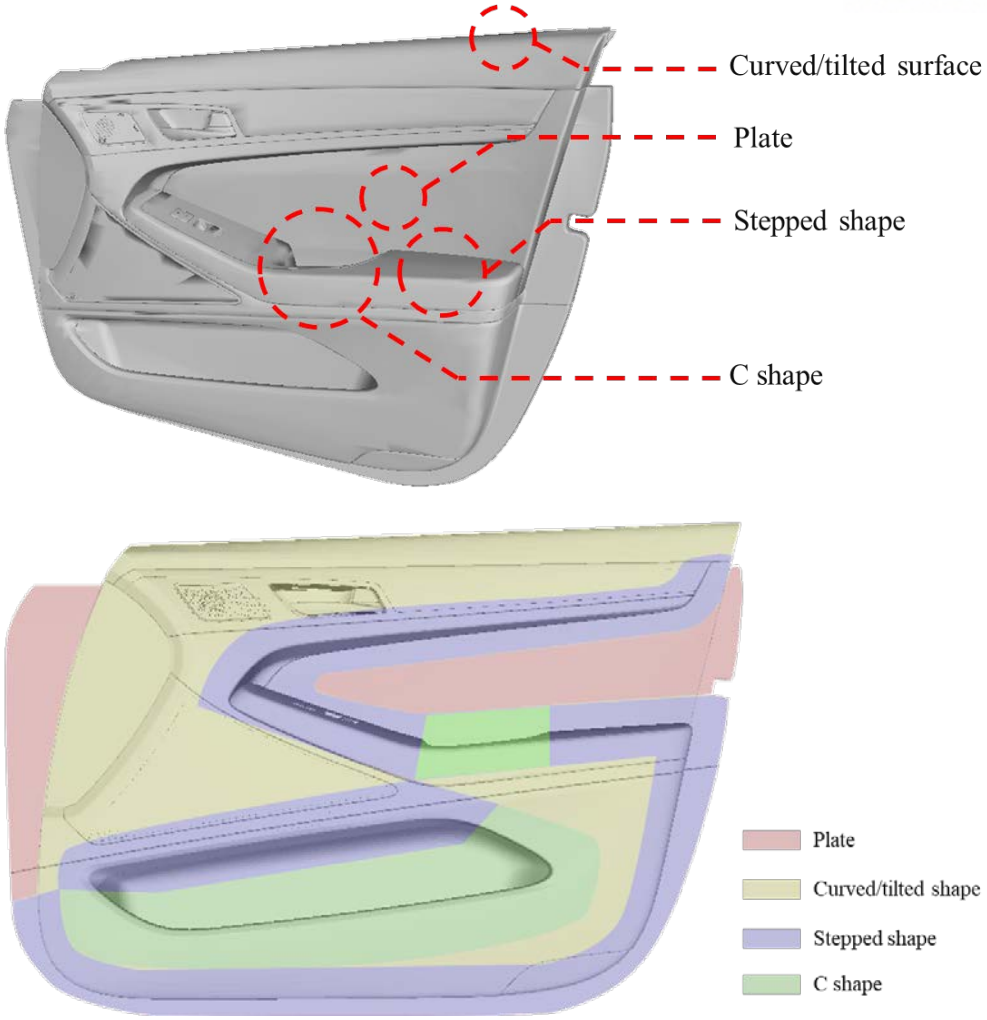

Figure 4. 5 Examples of shape types

For the experiment, I had simplified those shape and conducted finite element analysis with simplified shapes. The following figure shows that simplified shapes for experiment. In these experiments, I compared the deformation of various shapes and prioritized those shapes to select which position is better for support. The followings are assumptions for experiments.

i. Finite element analysis is conducted under conditions with isoparametric and linear

ii. The external forces are proportional to x-y plane and has same values

iii. All the shapes is composed of same materials

iv. The deformation is influenced by shape, thickness, distance between support and external force

v. Interest area of deformation is location of external force because it is on assembly joint point

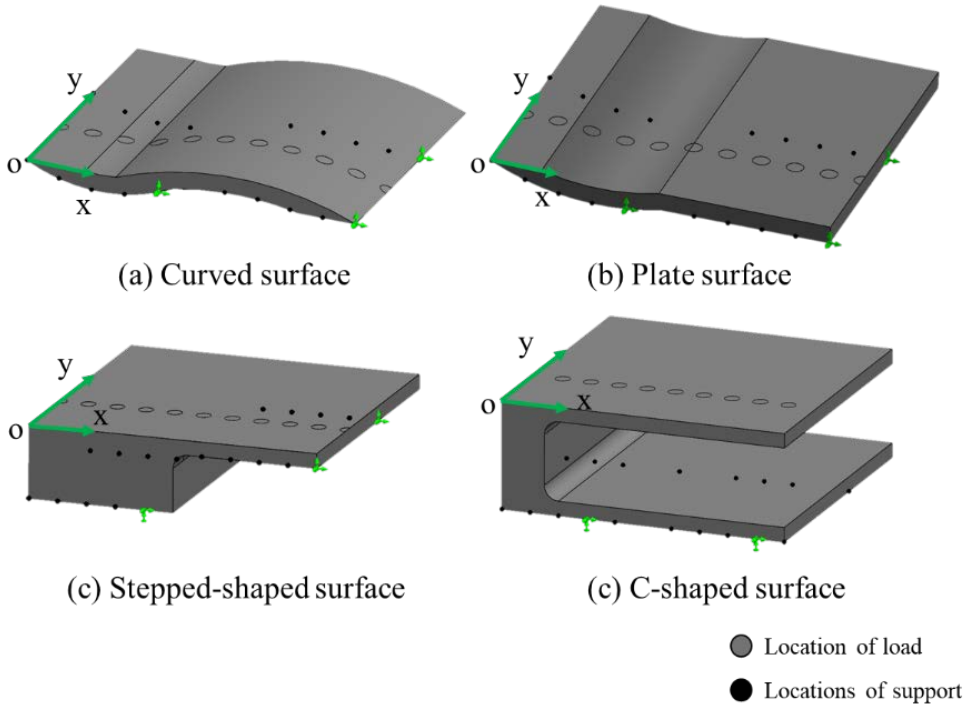

Figure 4. 6 Design of experiments

These experiment have four support points and one external load on each step. Each step has an external load with a different distance from the origin and support points with different distances from the origin. Total number of external load is nine and total number of support points is five. So each experiment have forty-five deformation data. Table 4. 3 shows the deformation data organized with making the origin the point of support point so that the deformation is not affected by the distance between support points and external load.

The table shows the deformation results in the order of (a), (b), (c) and (d) of figure 4. 5. On the first table 4. 3, deformations of surface with less curvature are bold letter. Compared with when supporting a less curved surface, it is less deformed by 59% on average when a more curved surface is supported. The radius of left curvature is 100 and radius of right curvature is 200.

On the (b) plate surface, deformations of plate are bold letter on the second table 4. 2. Compared with when supporting a flat part, it is less deformed by 9% when the part with curvature is supported on average.

On the third table, bold letter deformations have same gap between supporting points and external load. The difference between two deformations is support location. The deformation when supporting points are supporting L-shape is smaller than that of not supporting L-shape by 25%.

On the fourth table 4. 3, deformations of C-shape surface are larger than deformations of curved surface by 66% on average. Bold letter deformations have same gap between supporting points and external load, but have different location of supporting points. The result shows that the deformation when supporting points are supporting a pillar is smaller than that of not supporting a pillar by 6%.

As shown the table 4. 3, C-shaped surface is most deformed, and the stepped-shaped surface is least deformed.

Table 4. 6 Deformation of finite element elements with curved surface within location of load

e \ f'	0	20	40	60	80
20	6.45E-02	1.60E-02	9.15E-03	7.71E-03	1.10E-02
40	3.92E-02	1.35E-02	9.52E-03	8.88E-03	**1.95E-02**
60	2.63E-02	1.27E-02	1.02E-02	**9.89E-03**	**3.28E-02**
80	1.74E-02	1.15E-02	**9.95E-03**	**1.13E-02**	**5.37E-02**
100	1.13E-02	**9.69E-03**	**1.05E-02**	**1.62E-02**	**9.21E-02**

f': distance between the origin ‘o’ and the closest jig points to ‘o’,
e: distance between the center of external load ‘c’ and the closest jig point to ‘c’

Table 4. 7 Deformation of finite element elements with plate surface within location of load

e \ f'	0	20	40	60	80
20	3.37E-02	1.21E-02	8.84E-03	8.12E-03	8.44E-03
40	2.13E-02	1.31E-02	1.11E-02	9.80E-03	**1.08E-02**
60	1.65E-02	1.41E-02	1.19E-02	**1.10E-02**	**1.27E-02**
80	1.34E-02	1.28E-02	**1.13E-02**	**1.13E-02**	**1.41E-02**
100	1.02E-02	**1.04E-02**	**1.04E-02**	**1.17E-02**	**1.81E-02**

f': distance between the origin ‘o’ and the closest jig points to ‘o’,
e: distance between the center of external load ‘c’ and the closest jig point to ‘c’

Table 4. 8 Deformation of finite element elements with stepped-shaped surface within location of load

e \ f'	0	20	40	60	80
20	1.15E-03	8.22E-04	8.64E-04	9.58E-04	**1.24E-03**
40	1.05E-03	9.99E-04	1.22E-03	1.55E-03	2.66E-03
60	1.08E-03	1.36E-03	1.86E-03	2.83E-03	4.91E-03
80	1.25E-03	1.93E-03	3.01E-03	4.63E-03	7.68E-03
100	**1.66E-03**	3.00E-03	4.74E-03	6.89E-03	1.26E-02

f': distance between the origin 'o' and the closest jig points to 'o',
e: distance between the center of external load 'c' and the closest jig point to 'c'

Table 4. 9 Deformation of finite element elements with C-shaped surface within location of load

e \ f'	0	20	40	60	80
20	3.07E-03	5.76E-03	1.26E-02	3.58E-02	**6.61E-02**
40	7.95E-03	1.59E-02	3.30E-02	7.55E-02	1.29E-01
60	1.73E-02	3.45E-02	6.69E-02	1.36E-01	2.19E-01
80	3.44E-02	6.50E-02	1.20E-01	2.21E-01	3.42E-01
100	**6.21E-02**	1.12E-01	1.94E-01	3.35E-01	5.03E-01

f': distance between the origin 'o' and the closest jig points to 'o',
e: distance between the center of external load 'c' and the closest jig point to 'c'

The above results can be summarized as following table 4. 5. The weight value is the normalized value. A shape with high value should be sufficient to support the position of the corresponding feature when placing the part on the pin-jigs

Table 4. 10 The priority of shapes

	Weight value
Concave surface	-0.305
Convex surface	-0.423
Plate surface	-0.256
Stepped-shaped surface	-0.768
C-shaped surface	1.753

V. Force and Deformation Estimation for Optimal Part Positioning

For reducing error while machining in an assembly process, the consideration of location and support of part is necessary. Location and support of part are related with each other. For getting an optimal solution of part position, both should be simultaneously calculated, using machining force of the assembly process.

Another important variable for reducing error is shape of a part and jig. The shape of the part is variable but our pin-jig is not variable. The features we can get from 3D mesh are various. NOOR et al. (1977) introduced a function related with curved beams having curvature. In addition, normal vector at some mesh cell can affect the part stability concern with external forces.

With the chapter 3, 3D jig shape transformer calculates initial part positioning and basic variables for optimal part positioning. In this chapter, I conduct some experiments to estimate the relationship between shapes of a part and the deformation/force.

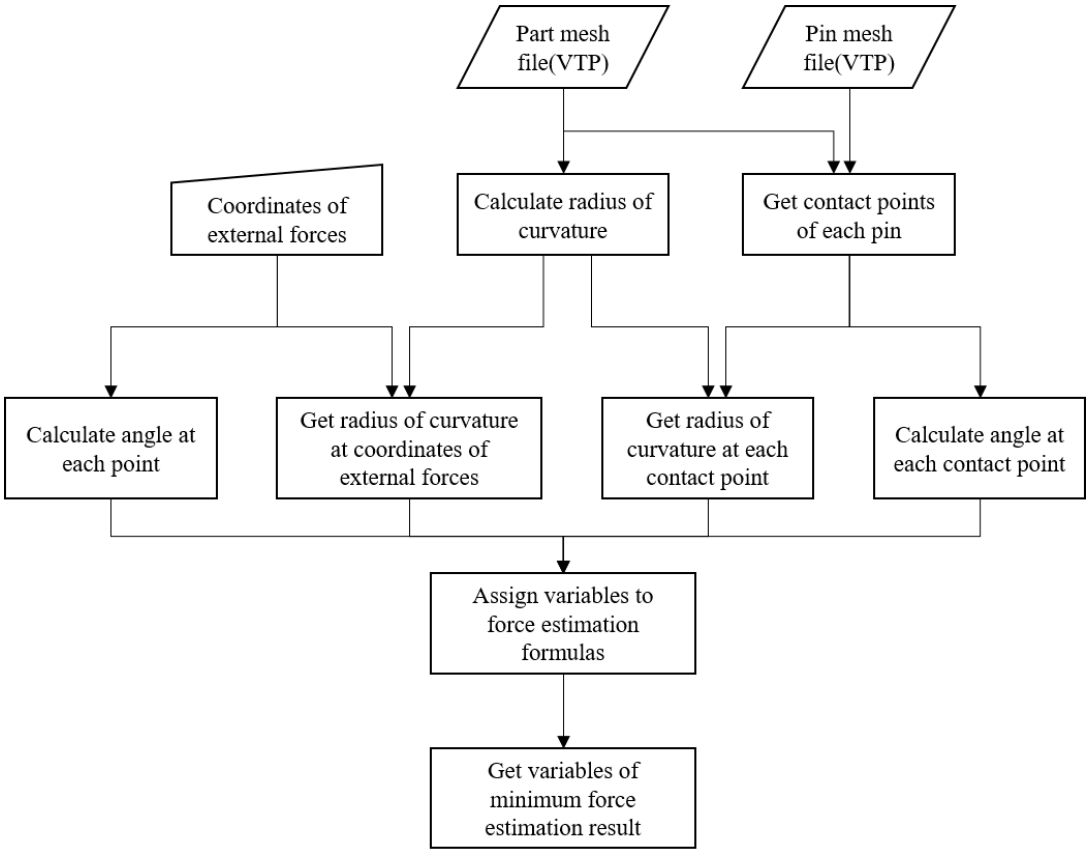

Figure 5. 1 Flow chart of geometric feature-based optimization for part positioning

5.1 Geometric feature-based Von mises stress and deformation estimation

In a 3D solid model, we can extract various geometric features such as type of element, resolution, contact point, curvature, angle of tangent, etc. To see a partial section, handling a point is necessary. For points only, significant features we can use are curvature and angle of tangent at a point. Using these variables, I conduct FEA experiments to find relationships that are Von mises stress-curvature, deformation-curvature, Von mises stress-angle of tangent, and deformation-angle of tangent.

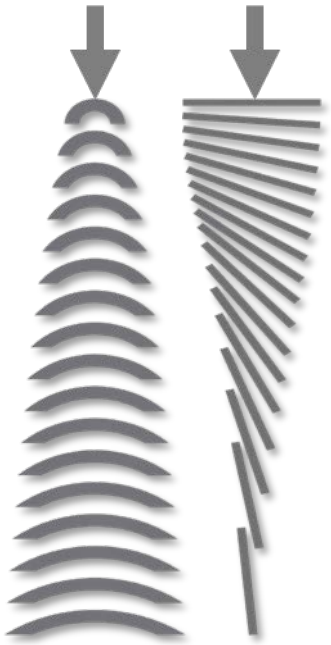

Figure 5. 2 Design of experiments with curvature and angle of tangent

The first experiment is about curvature of part. As radius of curvature increased, the maximum Von mises stress is increased as shown figure. 5. 3. Correlation coefficients between them is like table 5. 1. The correlation coefficient related with force is larger than that related with deformation. When the x-axis is concerned about curvature, the trend of maximum y displacement shows form of quadratic expression. But when the x-axis is concerned about radius of curvature, the trend of maximum y displacement comes to the form of linear expression. Therefore, it is more useful to use the radius of curvature as a parameter when creating an estimation equation.

And for the normal force, the angle is parameter of determining amplitude of normal force. As degree increased, the maximum Von mises stress is decreased. The correlation coefficient between them is like in this table 5. 2.

The trend about maximum y displacement related with radius of curvature shows linear form. However, the trend about angle of tangent does not shows linear form. On the contrary, both trends about maximum von-mises stress shows linear form. That is why I used maximum von-mises stress for making estimation model.

Both result shows that Von mises stress is more related with curvature. Based on above results of experiments, I conduct experiment with both variables. After that, built an estimation model with regression. The experiment shows the model is close to quadratic equation than linear one as shown Figure. 5. 4. The FEA experiments were conducted 45 times according to radius of curvature and tilted angle of plate.

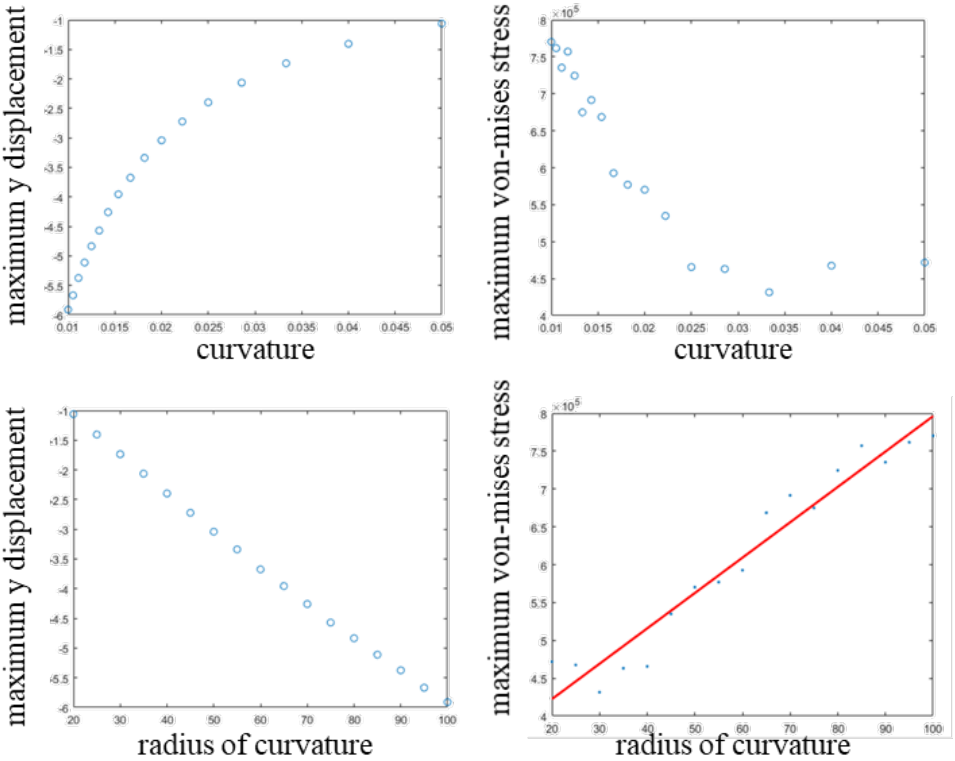

Figure 5. 3 Force-curvature and deformation-curvature analysis

Table 5. 1 Correlation coefficient between curvature and force/deforamtion

Variable	Correlation coefficient
Y-axis displacement	0.9204
Force	-0.9992

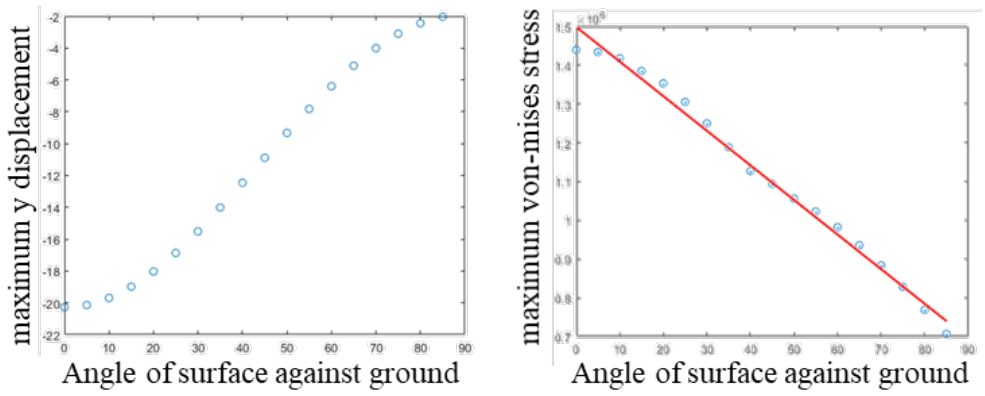

Figure 5. 4 Force-normal vector and deformation-normal vector analysis

Table 5. 2 Correlation coefficient between angle of plate and force/deforamtion

Variable	Correlation coefficient
Force	0.9928

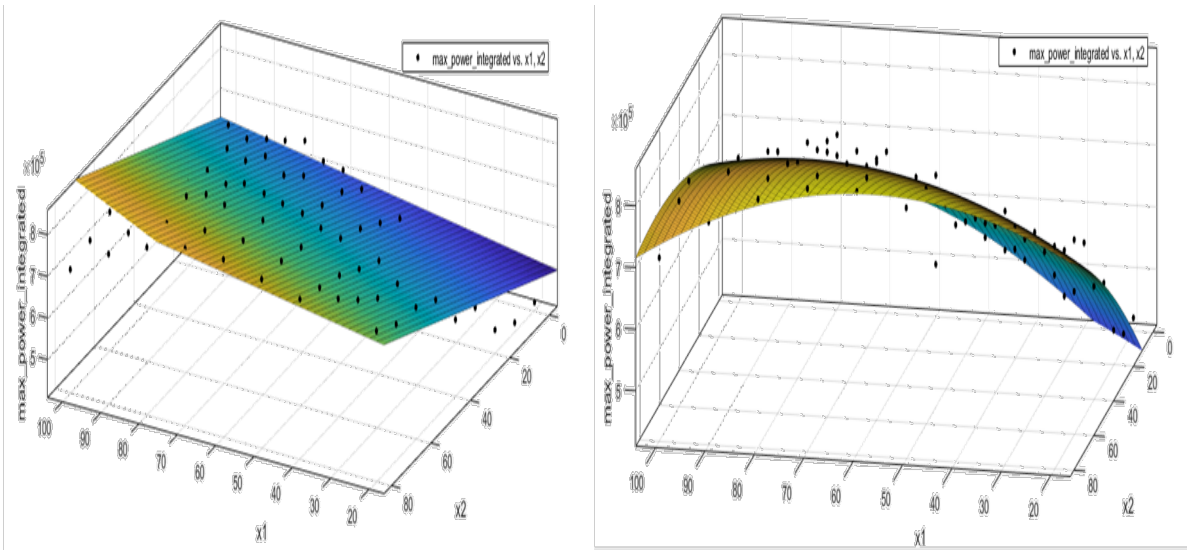

Figure 5. 5 Regression models of Von mises stress and curvature/normal vector

The equation of linear regression model is

$$F(x,y) = p_{00} + p_{10}x + p_{01}y$$

where, p_{00} is 4.844e+05, p_{10} is 1532, and p_{01} is 3087. The r-square of linear regression model is 0.7407. x1 of Fig. 6. 3 is radius of curvature and x2 is tilted angle of plate.

The equation of quadratic regression model is

$$F(x,y) = p_{00} + p_{10}x + p_{01}y + p_{20}x^2 + p_{11}xy + p_{02}y^2$$

where p_{00} is 1.902e+05, p_{10} is 1.005e+04, p_{01} is 7629, p_{20} is -55.8, p_{11} is -45.6, p_{02} is -22.57. The r-square of quadratic regression model is 0.9431. Equation of higher order has lower r-square than that of quadratic equation. Therefore, it is meaningful to used quadratic regression model.

To optimize a position of part on pin-jigs in assembly process, Manufacturers have to consider that joint point on pin-jigs. A joint point is section that receives external force and connect parts. Because pin-jigs support parts with points of pin-jig head, the boundary condition consists of points. Therefore, I conduct an experiment related with supporting points and location of external force. A purpose of the experiment is find the smallest deformation according to different locations of external forces.

The experiment observe the deformation when external force press certain point that is joint point. For the observation of the assembly part, two plates partially overlapped each other as shown Figure. 5. 4. In each experiment, the location of external force changes according to the distance between a pin-jig and an external force.

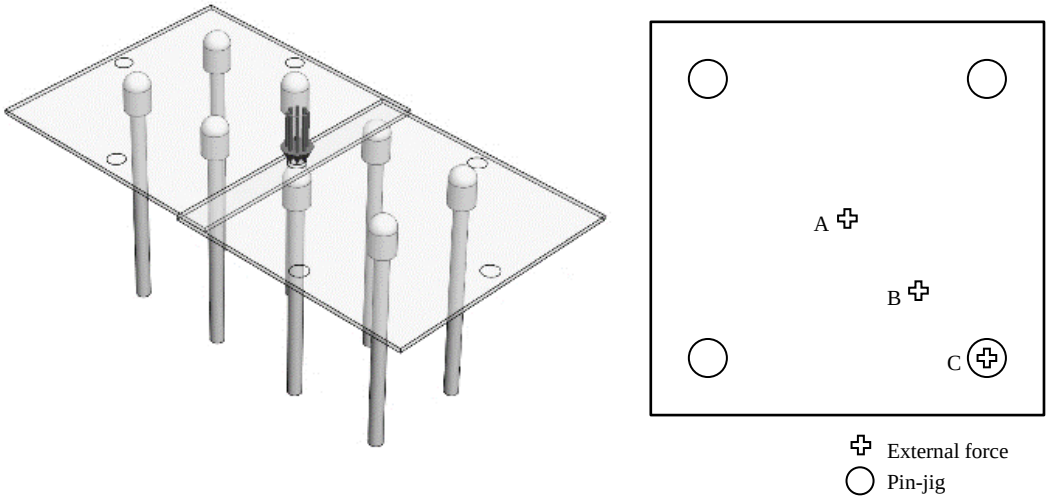

Figure 5. 6 Experiment setup for observe the deformation of an assembly part

The result of commercial FEM software calculate the deformation as shown Figure. 5. 7 and Table 5. 3.

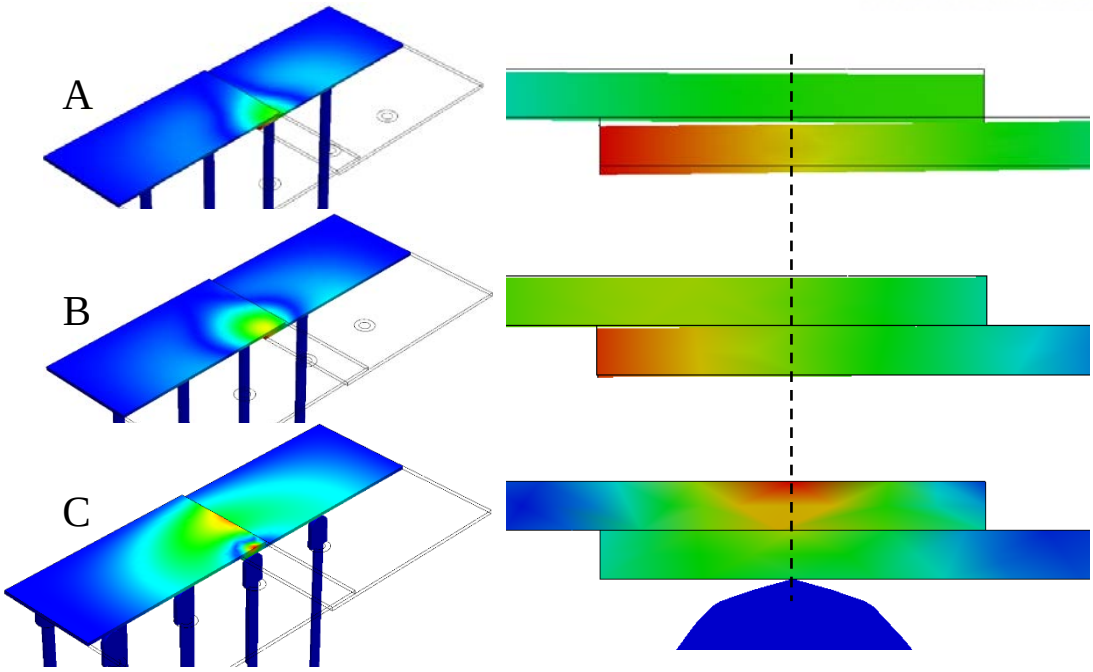

Figure 5. 7 Result of toy problem experiment

Table 5. 3 Result of toy problem experiment

Symbol	Dist.(mm)	Max. URES(mm)
A	84.8	8.992e-1
B	42.4	3.191e-1
C	0	2.670e-3

Finally, I can make a estimation model to find optimal part positioning with those results of experiments.

$$Min \sum \left\| \frac{f_c(\kappa_{ci},\ \theta) \cdot dist(P_{exfi}, C_{pj})}{n} \right\|$$

S.T

$P_{exfi} = [x_{exfi},\ y_{exfi},\ z_{exfi}]$ i = 1,2,3 …, P_{exf} is center coordinates of a contact force, $P = [P_{exf1},\ P_{exf2},\ P_{exf3},\ \ldots]$, $C_{pi} = [x_{pi},\ y_{pi},\ z_{pi}]$, i = 1, 2, 3 …, C_p is a center of a pin-jig, $C_{pi} = C_{p(i-1)} + [\alpha,\ \alpha,\ 0]$, All pin-jig are arranged with equal interval, κ_{ci} is curvature of surface at contact points, n is the number of contact points, θ is angle of normal vector, $f_c(\kappa_{ci},\ \theta)$ = p00 + p10· $\frac{1}{\kappa_{ci}}$ + p01·y + p20· $\frac{1}{\kappa_{ci}^2}$ + p11· $\frac{1}{\kappa_{ci}} \cdot \theta$ + p02· θ^2, $dist(P_{exfi}, C_{pj})$ is shortest distance from P_{exfi} to C_{pj}.

5.2 Optimal part positioning experiment

With above estimation model, I conduct an experiment to solve optimal part positioning of toy model. The boundary is fixed at four corner of the part. When viewed from above, all pin-jigs that can contact the part were contacted and fixed. The figure 5.8 shows the design of experiment in commercial FEA software.

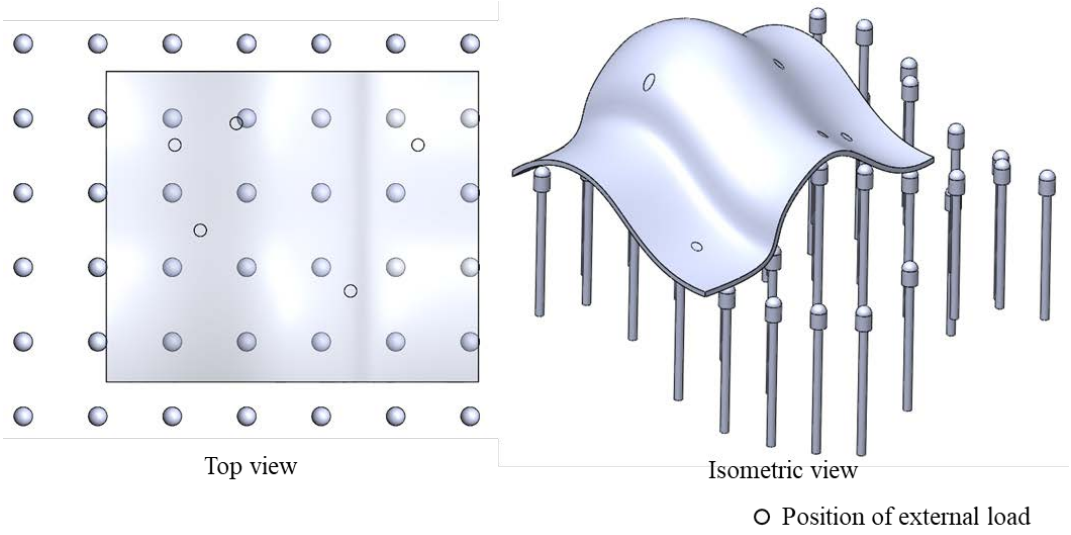

Figure 5. 8 Initial position of experiment with toy model in commercial software

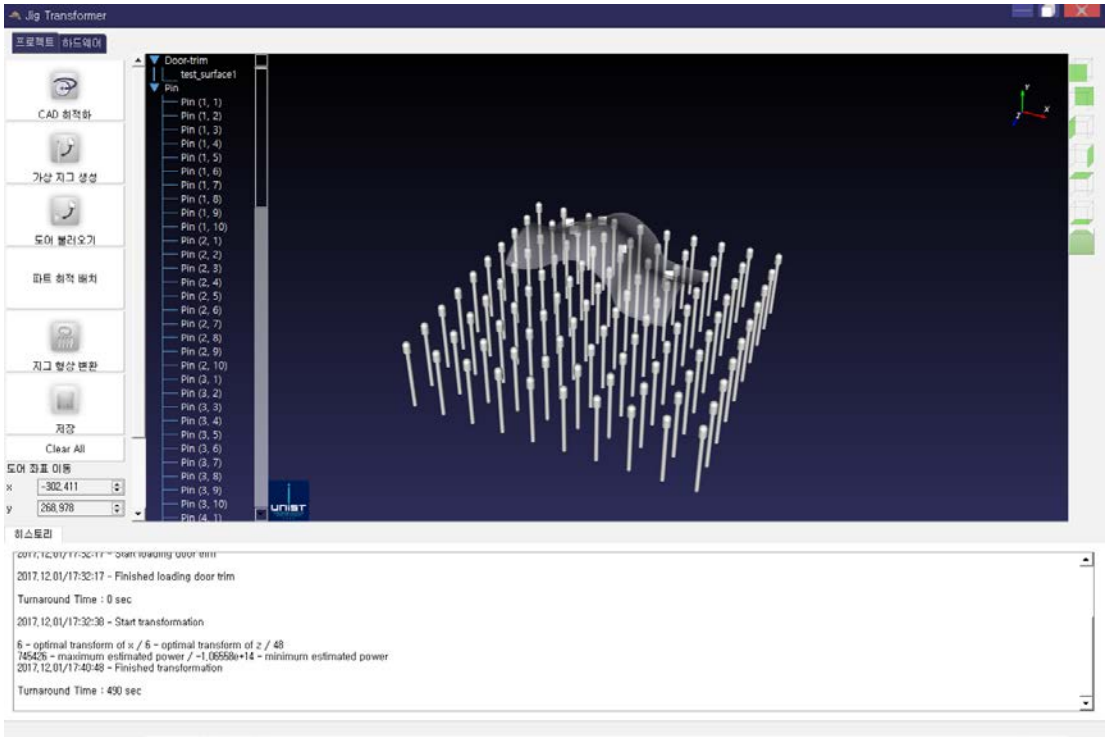

Figure 5. 9 Initial position of experiment with toy model in 3D jig shape transformer

Then set the 3D jig shape transformer to have the same conditions with commercial software. The result of estimation model is least deformation result when the part moved +60mm along with x and y-axis from initial position.

The following figure 5. 10 and table 5. 4 shows the result of FEA. The average von-mises stress and deformation at optimized position is less than that of initial position. Moreover, the maximum von-mises stress at optimized position is less than that of initial position. These estimated values from the estimation model has error rate of 14% on average, when it is compared to result of commercial FEA software.

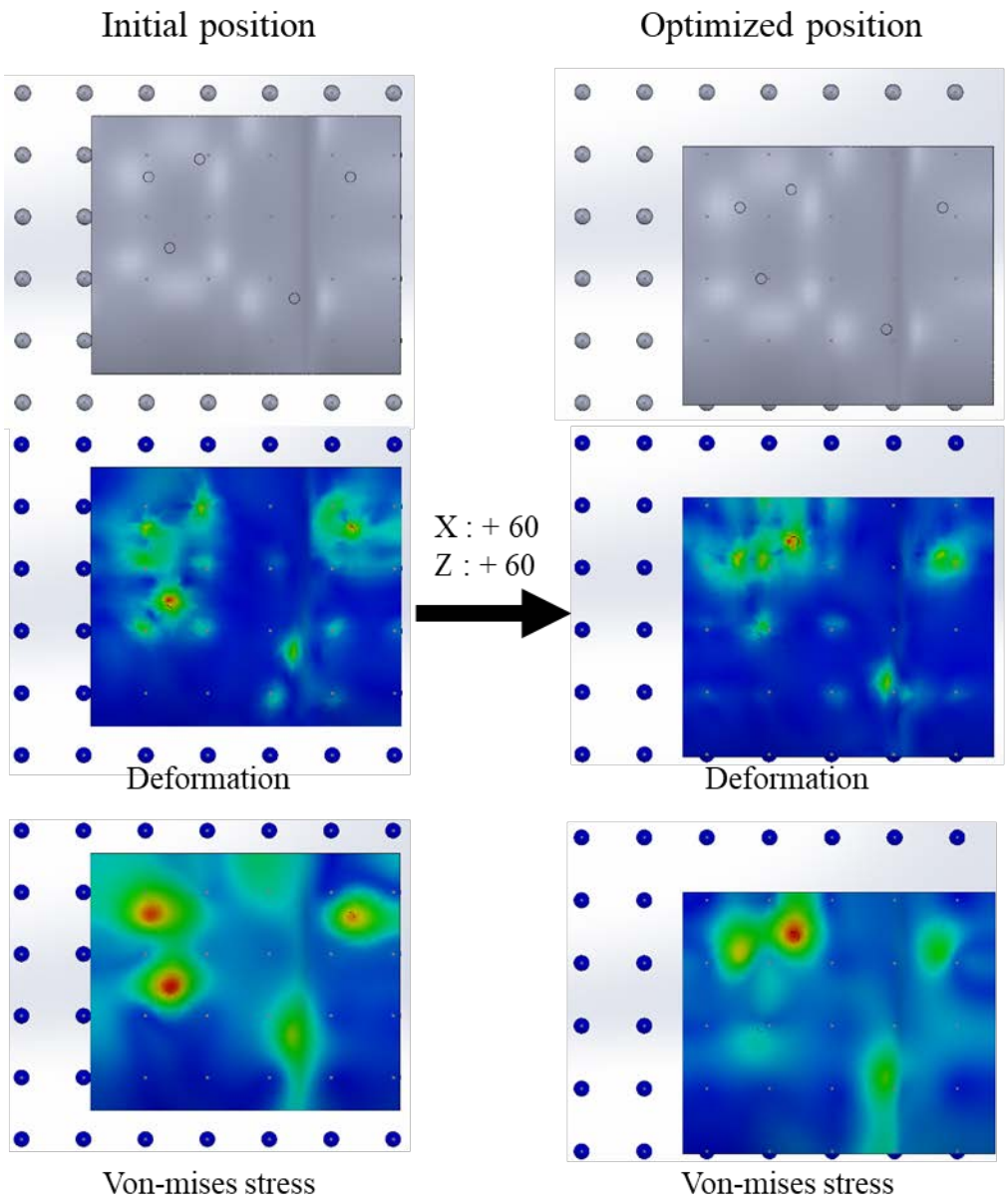

Figure 5. 10 Result of FEA of the initial part and the moved part

Table 5. 4 Average von-mises and deformation result

	Initial position (N/m^2)	Optimized position (mm)
Average von-mises	2.150e+4	1.730e+4
Average displacement	1.120e+1	7.790e-1
Maximum von-mises	8.680e+5	7.454e+5

VI. Conclusion and Future Research

In this study, a reconfigurable pin-jig system, consisting of (i) reconfigurable pin-jigs (Section 3.2.1) and (ii) a 3D pin-jig shape transformer (Section 3.2.2) was implemented. The purpose of this system is to provide a jig that can fix parts during assembly in the assembly line and support shapes that fit into various types of parts without having to replace the jig. In order to transform its shape freely, a jig hardware that can be changed into various shapes and a software that can calculate the stroke of the pin-jig were developed.

The reconfigurable pin-jigs were made after several trials and errors. The first one was to control the stroke of the pin-jig. First, an ultrasonic sensor was used to find out how long the stroke moved with the DC motor. However, the accuracy of the ultrasonic sensor was low, and it was difficult to control the DC motor. To solve these problems, a servo motor was used. In addition, the prototype was made using hardware that can mount all the pin-jigs and motor drive parts on the wide plate; however, owing to the difficulties in maintenance, it was changed to the current modular form.

The 3D pin-jig shape transformer, which is the name of the control software, calculates the strokes of pin-jigs using the 3D CAD of the pin-jig and a part. After that, the reconfigurable pin-jigs receive the results of the strokes and execute the command. In the 3D pin-jig shape transformer, a geometric feature-based stress and deformation estimation model calculates the optimal position for the part. The estimation model is based on the results of finite element analysis. The curvature and angle are important variables in the estimation model.

The geometric feature-based stress and deformation estimation model for the optimal assembly part positioning is suitable for finding the location of a part on a reconfigurable pin-jig, assuming that the assembly process are subjected to only transverse forces. However, if there are non-transverse forces, it can be more complicated to calculate the optimal position of a part. In future, not only the transverse pressure on a part, but also other forces would be calculated to develop a more general estimation model. Validation of the finite element method is recommend using real assembly processes.

It was initially assumed that the error is not significant and that the trend of the estimated result is similar to the trend of finite element analysis result, so that the deformation of a part could be estimated. Therefore, this research is based on linear and isoparametric finite element analysis. In the case of non-linear or nonisoparametric finite element analysis, the estimation equation becomes more complicated, but the error rate can be lowered. Moreover, it was assumed that the boundary condition consists of

only four points. However, the actual boundary condition includes the contact surface between the pin-jigs and a part. To solve this problem, the contact finite element method should be considered.

References

1. Attila, R., Stampfer, M., & Imre, S. (2013). Fixture and Setup Planning and Fixture Configuration System. *Procedia CIRP, 7*, 228-233. doi:10.1016/j.procir.2013.05.039
2. Bin, J., & Wanji, C. (2010). A new analytical solution of pure bending beam in couple stress elasto-plasticity: Theory and applications. *International Journal of Solids and Structures, 47*(6), 779-785. doi:10.1016/j.ijsolstr.2009.11.011
3. Bone, G. M., & Capson, D. (2003). Vision-guided fixtureless assembly of automotive components. *Robotics and Computer-Integrated Manufacturing, 19*(1-2), 79-87. doi:10.1016/s0736-5845(02)00064-9
4. Cook, N. J., Smith, G. F., & Maggs, S. J. (2008). A Novel Multipin Positioning System for the Generation of High-Resolution 3-D Profiles by Pin-Arrays. *IEEE Transactions on Automation Science and Engineering, 5*(2), 216-222. doi:10.1109/tase.2007.894725
5. ElMaraghy, H. A. (2006). Flexible and reconfigurable manufacturing systems paradigms. *International Journal of Flexible Manufacturing Systems, 17*(4), 261-276. doi:10.1007/s10696-006-9028-7
6. Follmer, S., Leithinger, D., Olwal, A., Hogge, A., & Ishii, H. (2013). inFORM: Dynamic Physical Affordances and Constraints through Shape and Object Actuation. 417-426. doi:10.1145/2501988.2502032
7. Fuwen, H. (2014). Location Issues of Thin Shell Parts in the Reconfigurable Fixture for Trimming Operation. *Journal of Aerospace Technology and Management, 6*(3), 319-331. doi:10.5028/jatm.v6i3.321
8. Gameros, A., Lowth, S., Axinte, D., Nagy-Sochacki, A., Craig, O., & Siller, H. R. (2017). State-of-the-art in fixture systems for the manufacture and assembly of rigid components: A review. *International Journal of Machine Tools and Manufacture, 123*, 1-21. doi:10.1016/j.ijmachtools.2017.07.004
9. Im, Y.-T., Walczyk, D. F., Schwarz, R. C., & Papazian, J. M. (2000). A Comparison of Pin Actuation Schemes for Large-Scale Discrete Dies. *Journal of Manufacturing Processes, 2*(4), 247-257. doi:10.1016/s1526-6125(00)70026-0
10. Jonsson, M., & Ossbahr, G. (2010). Aspects of reconfigurable and flexible fixtures. *Production Engineering, 4*(4), 333-339. doi:10.1007/s11740-010-0256-z
11. Junbai, L., & Kai, Z. (2010). Multi-point location theory, method, and application for flexible tooling system in aircraft manufacturing. *The International Journal of Advanced Manufacturing Technology, 54*(5-8), 729-736. doi:10.1007/s00170-010-2974-y
12. Koren, Y., & Shpitalni, M. (2010). Design of reconfigurable manufacturing systems. *Journal of Manufacturing Systems, 29*(4), 130-141. doi:10.1016/j.jmsy.2011.01.001
13. Kuo, Y. L., & Cleghorn, W. L. (2010). Curvature- and displacement-based finite element analyses of flexible four-bar mechanisms. *Journal of Vibration and Control, 17*(6), 827-844. doi:10.1177/1077546309353917
14. Levy, G. N., Schindel, R., & Kruth, J. P. (2003). Rapid Manufacturing and Rapid Tooling with Layer Manufacturing (Lm) Technologies, State of the Art and Future Perspectives. *CIRP Annals, 52*(2), 589-609. doi:10.1016/s0007-8506(07)60206-6
15. Li, B., Xu, P., Yu, H., Lou, Y., & Yang, X. (2015). *Design and Analysis of Parallel Robots for a Flexible Fixturing System with Performance Atlases*. Paper presented at the 2015 IEEE/RSJ International Conference on Intelligent Robots and Systems (IROS), Hamburg, Germany.
16. Logan, D. L. (2016). *A First Course in the Finite Element Method*: Cengage Learning.
17. Molfino, R., Zoppi, M., & Zlatanov, D. (2009). *Reconfigurable Swarm Fixtures*. Paper presented at the Reconfigurable Mechanisms and Robots, 2009. ReMAR 2009. ASME/IFToMM International Conference on, London.
18. Moroni, G., Petrò, S., & Polini, W. (2014). Robust Design of Fixture Configuration. *Procedia CIRP, 21*, 189-194. doi:10.1016/j.procir.2014.03.120

19. Munro, C., & Walczyk, D. (2007). Reconfigurable Pin-Type Tooling: A Survey of Prior Art and Reduction to Practice. *Journal of Manufacturing Science and Engineering, 129*(3), 551. doi:10.1115/1.2714577
20. NOOR, A. K., GREENE, W. H., & HARTLEY, S. J. (1977). NONLINEAR FINITE ELEMENT ANALYSIS OF CURVED BEAMS. *In Computer Methods in Applied Mechanics and Engineering, 12*(3), 289-307. doi:https://doi.org/10.1016/0045-7825(77)90018-4
21. Olaiz, E., Zulaika, J., Veiga, F., Puerto, M., & Gorrotxategi, A. (2014). Adaptive Fixturing System for the Smart and Flexible Positioning of Large Volume Workpieces in the Wind-power Sector. *Procedia CIRP, 21*, 183-188. doi:10.1016/j.procir.2014.03.193
22. Peters, B. J. (2013). *Practical Pin Tooling.* (Master), Massachusetts Institute of Technology,
23. Rong, Y., Huang, H, S., & Hou, Z. (2005). *Advanced computer-aided fixture design*. Amsterdam: Elsevier.
24. Siebenaler, S. P., & Melkote, S. N. (2006). Prediction of workpiece deformation in a fixture system using the finite element method. *International Journal of Machine Tools and Manufacture, 46*(1), 51-58. doi:10.1016/j.ijmachtools.2005.04.007
25. Simon, D., Kern, L., Wagner, J., & Reinhart, G. (2014). A Reconfigurable Tooling System for Producing Plastic Shields. *Procedia CIRP, 17*, 853-858. doi:10.1016/j.procir.2014.01.095
26. T.Patil, A., S.M.Pise, S.G.Bhatwadekar, & S.B.Sangale. (2015). various flexible fixturing systems in manufacturing-a review. *IJIRSET, 4*(9), 8440-8444. doi:10.15680/IJIRSET.2015.0409064
27. Wang, H., Rong, Y., Li, H., & Shaun, P. (2010). Computer aided fixture design: Recent research and trends. *Computer-Aided Design, 42*(12), 1085-1094. doi:10.1016/j.cad.2010.07.003
28. Xu, J., Sun, Y., & Wang, S. (2012). Tool path generation by offsetting curves on polyhedral surfaces based on mesh flattening. *The International Journal of Advanced Manufacturing Technology, 64*(9-12), 1201-1212. doi:10.1007/s00170-012-4075-6
29. Xuemei, H. (2009). Intelligent and Reconfigurable Control ofAutomatic Production Line by Applying IEC61499 Function Blocks and Software Agent. *Proceedings of the 2009 IEEE International Conference on Mechatronics and Automation*.
30. YAMADA, T., YAMADA, M., & YAMAMOTO, H. (2011). Stability Analysis of A Single Object Grasped by A Multifingered Hand with Angular Joints in 2D. *Proceedings of the 2011 IEEE International Conference on Mechatronics and Automation*.
31. Yang, F., Gao, K., Simon, I. W., Zhu, Y., & Su, R. (2018). Decomposition methods for manufacturing system scheduling: a survey. *IEEE/CAA Journal of Automatica Sinica, 5*(2), 389-400. doi:10.1109/jas.2017.7510805
32. Zhang, Z., Tendulkar, A., Sun, K., Saloner, D. A., Wallace, A. W., Ge, L., . . . Ratcliffe, M. B. (2011). Comparison of the Young-Laplace law and finite element based calculation of ventricular wall stress: implications for postinfarct and surgical ventricular remodeling. *Ann Thorac Surg, 91*(1), 150-156. doi:10.1016/j.athoracsur.2010.06.132